ACR No. L4I20

NATIONAL ADVISORY COMMITTEE FOR AERONAUTICS

WARTIME REPORT

ORIGINALLY ISSUED
September 1944 as
Advance Confidential Report L4I20

THE PROPELLER AND COOLING-AIR-FLOW CHARACTERISTICS OF A TWIN-ENGINE AIRPLANE MODEL EQUIPPED WITH NACA D_S-TYPE COWLINGS AND WITH PROPELLERS OF NACA 16-SERIES AIRFOIL SECTIONS

By James G. McHugh and Edward Pepper

Langley Memorial Aeronautical Laboratory
Langley Field, Va.

NACA

WASHINGTON

NACA ACR No. L4I20 CONFIDENTIAL

NATIONAL ADVISORY COMMITTEE FOR AERONAUTICS

ADVANCE CONFIDENTIAL REPORT

THE PROPELLER AND COOLING-AIR-FLOW CHARACTERISTICS OF A TWIN-ENGINE AIRPLANE MODEL EQUIPPED WITH NACA D_S-TYPE COWLINGS AND WITH PROPELLERS OF NACA 16-SERIES AIRFOIL SECTIONS

By James G. McHugh and Edward Pepper

SUMMARY

An investigation was conducted in the NACA 19-foot pressure tunnel to determine the nacelle drag, the cowling-air flow, and the propeller characteristics of a model of a high-performance military airplane. The airplane model, which is approximately one-quarter scale, is fitted with NACA D_S-type engine cowlings and with propellers embodying NACA 16-series airfoil sections. The characteristics of the propellers were determined through a range of blade angles from 20° to 60°, and a brief study was made of the effects of variations of angle of attack and cowling-flap deflection on the propeller characteristics. The variations of nacelle drag and internal air flow obtained with various arrangements of cowling flaps and variable-length cowling skirts, as well as the effect of the operating propeller on the internal-flow characteristics, were also determined.

The results of the investigation indicate that: (1) the propulsive efficiency of the propeller tested varied from 88 percent at a value of advance-diameter ratio of 0.8 to nearly 93 percent at a value of advance-diameter ratio of 2.4 and gradually decreased to about 89 percent at a value of advance-diameter ratio of 3.8; (2) in the range of internal-flow rate attainable with a variable-length skirt, the parasite drag of the nacelle when fitted with this arrangement is moderate and is about equal in magnitude to the parasite drag of the nacelle when equipped with adjustable cowling flaps; (3) the parasite drag of nacelles, equipped with cowling

flaps of approximately the same proportions as those investigated, does not increase appreciably with cowling-flap deflections of 12° or less; (4) in order to obtain the pressure drop necessary to provide satisfactory engine cooling, well-designed cowling flaps may be deflected to angles in excess of 12° at the expense of rapidly increasing the drag; hence, the performance of an airplane equipped with such an arrangement may in certain instances be penalized; (5) although cowling flaps provide a powerful means for obtaining adequate cooling at the ground and for take-off, such air flow is not attainable for nacelles equipped with variable-length cowling skirts.

INTRODUCTION

Information concerning the characteristics of propellers that embody the recently developed NACA high-speed airfoil sections operating in conjunction with modern air-cooled radial-engine cowlings is meager. The literature that is available has been obtained from tests of isolated nacelle-propeller combinations. No data has heretofore been available concerning the characteristics of such arrangements operating in conjunction with a complete airplane.

Knowledge concerning the change in form drag of the nacelle that accompanies an increase in the rate of cowling-air flow when such increase is accomplished by the use of adjustable cowling flaps is also meager. Little data exist on the relative merits of adjustable cowling flaps and adjustable-length cowling skirts as a means of controlling the rate of air flow, although this subject has been treated to some extent in reference 1. The results presented, however, were obtained from tests at relatively low Reynolds number of an isolated nacelle fitted with an NACA C-type cowling and did not include sufficient measurements of the internal flow to permit accurate determination of either the internal drag or the average pressure drop through the cowling.

In order to provide additional information on this subject, the propeller and cooling characteristics of a model of a high-performance twin-engine military airplane have been investigated. The airplane model is approximately one-quarter scale, is fitted with NACA

D_S-type engine cowlings, and is equipped with propellers that embody NACA 16-series airfoil sections. Studies were made to determine (1) the thrust, power, and efficiency characteristics of the propellers; (2) the relative merits of cowling flaps and variable-length cowling skirts as a means of controlling the cooling-air flow; and (3) the drag characteristics of the nacelle.

SYMBOLS AND COEFFICIENTS

The symbols and coefficients involved are defined as follows:

A	cowling-duct area
α	angle of attack of thrust line
A_n	nacelle cross-sectional area (0.99 sq ft for model)
β	propeller blade angle at 0.75 tip radius
C_D	drag coefficient of airplane model (D/qS)
C_{D_F}	coefficient of internal drag of one nacelle
C_{D_n}	total nacelle drag coefficient (D_n/qA_n)
$C_{D_{n_o}}$	nacelle parasite-drag coefficient ($C_{D_n} - C_{D_F}$)
C_L	lift coefficient (L/qS)
C_T	thrust coefficient $\left(\frac{T - \Delta D}{\rho n^2 D^4}\right)$
C_P	power coefficient ($P/\rho n^3 D^5$)
C_s	speed-power coefficient $\left(\sqrt[5]{\frac{\rho V^5}{\rho n^2}}\right)$
D	drag of airplane model (propeller off)
ΔD	change in parasite drag of airplane model due to slipstream of one propeller
D_F	internal drag of one nacelle

D_n	total increment of drag due to one nacelle
D	diameter of propeller (2.969 ft for model)
F	engine cross-sectional area (0.8479 sq ft for model)
H	total pressure
K	conductivity of cowling $\left[Q/FV\left(\frac{\Delta p}{q}\right)^{\frac{1}{2}}\right]$
K_2	cowling-exit-area ratio $\left(\frac{\text{Cowling-exit area}}{\text{Nacelle cross-sectional area}}\right)$
L	lift
M_T	blade-tip Mach number $\left(\frac{\text{Resultant tip speed}}{\text{Sonic velocity}}\right)$
n	propeller rotational speed
η	propulsive efficiency $\left(\frac{(T - \Delta D)V}{P}\right)$
P	power input to one propeller
p	static pressure
$\frac{H_1 - H_o}{q_o}$	cowling-entrance total-pressure coefficient
$\frac{H_o - H_2}{q_o}$	cowling-exit total-pressure coefficient
Δp	pressure drop through cowling $(H_1 - H_2)$
q	dynamic pressure $\left(\frac{1}{2}\rho V^2\right)$
Q	quantity rate of air flow through cowling
ρ	air density
S	wing area (30.49 sq ft for model)
T	thrust of one propeller (tension in crankshaft)
T_c	thrust-loading coefficient $\left(\frac{T - \Delta D}{\rho V^2 D^2}\right)$

V velocity

V/nD advance-diameter ratio of propeller

Subscripts:

o free stream

1 cowling entrance

2 cowling exit

Free-stream conditions are also signified if no subscripts are used.

APPARATUS AND METHODS

The investigation was conducted in the NACA 19-foot pressure tunnel. The airplane model used in the investigation (fig. 1) is a 0.2375-scale model of a high-performance twin-engine military airplane. The engine cowlings were of the NACA D_S short-nose high-inlet-velocity type (reference 2) designed for the Pratt & Whitney R-2800 engine.

The general arrangement of the nacelle with cowling is shown in figure 2. Details of the nacelle are presented in figure 3. The resistance of the engine to the flow through the nacelle was simulated by a baffle inside the cowling. The conductivity of the cowling was determined from measurements of the quantity of air flow and of the pressure drop in the cowling. For this investigation the baffle that simulated the engine was adjusted to provide a value of conductivity of the cowling K of 0.125. In order to provide for varying the cowling-exit area, the skirt of the cowling was removable and could be replaced with alternate flared skirts to simulate adjustable cowling flaps. Control of the cowling-exit area was also obtained through the use of alternate unflared cowling skirts of various lengths. With the flared skirts, cowling-flap deflections of 0.5°, 5.5°, 11.0°, 15.5°, 20.5°, and 25.5° were obtained and with the unflared skirt, cowling-flap lengths of 3.25, 2.75, 2.25, 1.75, and 1.25 inches were obtained. The effect of the various cowling flaps and variable-length cowling skirts on the ratio of cowling-exit area to nacelle cross-sectional area is shown in figure 4.

The characteristics of the air flow through the cowling were determined from measurements of the pressures acting on shielded total-pressure tubes at the cowling entrance (station 1) and on unshielded total-pressure tubes near the cowling exit (station 2) as shown in figure 3. The pressures acting on the tubes were photographically recorded on a multiple-tube manometer.

The three-blade model propellers investigated were 2.969 feet in diameter and were geometrically similar to the full-scale 12.5-foot diameter, Hamilton Standard propeller 6457A-6. The blades (fig. 5) were of activity factor 87.1 and incorporated NACA 16-series sections with shank fairings built as an integral part. The blade-form curves showing the width, thickness, and pitch distribution are presented in figure 6. Each propeller was driven by a water-cooled induction motor capable of developing a maximum torque of 125 foot-pounds.

TESTS

The tests were conducted with the air in the wind tunnel compressed to 35 pounds per square inch and at airspeeds ranging up to 160 miles per hour.

For the tests with propellers operating the blades were set at 20°, 30°, 35°, 40°, 45°, 50°, 55°, and 60° at 0.75 of the tip radius. The tests were also made at several values of angle of attack of the model and of the several cowling-exit configurations. The model motors were controlled through a speed range of approximately 1500 to 4000 rpm. The power delivered to each propeller was obtained from a calibration involving torque, rotational speed, and motor current. The thrust produced by the propellers was determined from differences in drag-balance reading with and without the propellers operating. The values of V/nD, at which these measurements were determined, were varied by maintaining constant model motor speed in the proximity of maximum torque output and by gradually increasing the wind-tunnel airspeed. When maximum propulsive efficiency had been approximately attained, the airspeed was held constant and the propeller rotational speed was decreased by predetermined increments until negative thrust was reached.

The blade-tip Mach numbers obtained are presented in figure 7 and range from approximately 0.25 for $\beta = 60^{\circ}$ to 0.50 for $\beta = 20^{\circ}$. The average Reynolds number for the tests was approximately 0.4 of the Reynolds number for full-scale operation at sea level.

In addition to the measurements of the propeller characteristics, the investigation also included measurements, both with and without the propellers operating, of the effect of variation in the cowling-exit condition on the drag and on the internal-flow characteristics of the cowling. In order to establish a reference base from which to measure the drag increment chargeable to the nacelle, the lift and drag characteristics of the airplane model with the nacelles removed were also obtained. The scope of the tests with propellers operating is given in table I and with propellers removed in table II.

METHOD OF ANALYSIS

The three primary concerns relative to a propeller-nacelle combination are (1) the rate of internal flow through the cowling and the cost of that flow in drag, (2) the parasite drag of the nacelle, and (3) the propulsive efficiency of the combination. In this paper each of these items will be considered in turn.

Internal flow.- The quantity of flow through the cowling is defined in reference 3 as

$$Q = KFV\sqrt{(\Delta p/q_o)} \qquad (1)$$

The drag chargeable to such flow may be evaluated from considerations of the change in momentum of the air flowing through the cowling. Thus,

$$D_F = \rho_o Q(V_1 - V_w) \qquad (2)$$

where V_w is the final wake velocity of the air leaving the cowling after its static pressure has returned to that of the free stream. By applying Bernoulli's theorem

and assuming that the static pressure of the air passing through the propeller has returned to the free-stream value p_o at the cowling entrance, it can be shown that, when the propeller is operating in front of the cowling, the drag contributed by the internal resistance of the cowling may be expressed as

$$D_F = \rho_o Q \left[\left(\frac{H_1 - p_o}{\rho_1/2} \right)^{1/2} - \left(\frac{H_2 - p_o}{\rho_2/2} \right)^{1/2} \right] \tag{3}$$

By substituting the value of Q defined in equation (1) and introducing coefficients, the expression becomes

$$C_{D_F} = \frac{D_F}{q_o A_n} = \frac{\rho_o K F V_o}{q_o A_n} \left(\frac{\Delta p}{q_o} \right)^{1/2} \left[\left(\frac{H_1 - p_o}{\rho_1/2} \right)^{1/2} - \left(\frac{H_2 - p_o}{\rho_2/2} \right)^{1/2} \right] \tag{4}$$

At the values of pressure and velocity that existed during the investigation, the density of the air in the duct was nearly equal to that of the free stream. Assuming $\rho_1 = \rho_2 = \rho_o$ and simplifying equation (4) permits the coefficient of internal drag to be expressed as

$$C_{D_F} = \frac{2KF}{A_n} \left(\frac{\Delta p}{q_o} \right)^{1/2} \left[\left(\frac{H_1 - p_o}{q_o} \right)^{1/2} - \left(\frac{H_2 - p_o}{q_o} \right)^{1/2} \right] \tag{5}$$

At high-speed or high-altitude flight conditions, large changes in density are likely to occur. In such cases the simplifying assumption of constant density will lead to large errors in calculating the internal drag.

It is often of interest to know the ratio of the velocity of the air entering the cowling to the velocity of the free stream. This ratio may be determined by making equation (1) equal to the product of the entrance area and velocity

$$Q = A_1 V_1 = K F V_o \left(\frac{\Delta p}{q_o} \right)^{1/2}$$

or

$$\frac{V_1}{V_o} = \frac{KF}{A_1}\left(\frac{\Delta p}{q_o}\right)^{1/2} \tag{6}$$

Nacelle drag.- The value of the total drag of each nacelle is determined from the difference, at equal values of lift coefficient, between the drag coefficients of the airplane model with and without nacelles according to the following relation

$$C_{D_n} = \frac{S}{2A_n} C_{D_{\text{with nacelles}}} - C_{D_{\text{without nacelles}}} \tag{7}$$

The coefficient of parasite drag chargeable to each nacelle is in turn determined from the difference between the total nacelle drag and the drag chargeable to the internal air flow

$$C_{D_{n_o}} = C_{D_n} - C_{D_F} \tag{8}$$

Propulsive efficiency.- It is conventional to express the propulsive efficiency of an airplane propeller as

$$\eta = \frac{(T - \Delta D)V_o}{P} \tag{9}$$

The expression $(T - \Delta D)$ is the propulsive thrust of the propeller and may be evaluated as follows:

$$(T - \Delta D) = R + D \tag{10}$$

where R is the net force along the drag axis, obtained with the propeller operating, and D is the drag with the propeller removed.

When the propeller-nacelle combination is operating in proximity to a wing, the lift generated with the propeller operating is likely to differ from that generated at the same angle of attack with the propeller removed and, therefore, unless suitable precautions are taken in determining the propulsive thrust, an erroneous value of propulsive efficiency may be obtained. The action of the propeller, in addition, may be such as to alter the rate of internal air flow through the cowling and, unless the change in drag resulting from such modifications to the flow is accounted for, this effect will be reflected either as an increase or a decrease in the efficiency credited to the propeller.

Any change in the wing lift characteristics due to the action of the propeller has been accounted for, in working up the results of this investigation, by determining the value of D (from equation (10)) at the same lift coefficient as that at which the value of R was measured.

Suitable corrections have been made to the values of the propulsive efficiency and the thrust coefficient to bring them to the basis of equal cowling drag with and without propellers operating. The increment of drag due to the action of the propeller on the flow through the cowling is

$$\Delta D_F = q_o A_n \left(C_{D_F}{}_{\text{propeller on}} - C_{D_F}{}_{\text{propeller removed}} \right) \quad (11)$$

Accordingly, the propulsive thrust as defined by equation (10) has been corrected as follows:

$$(T - \Delta D) = R + D - \Delta D_F \quad (12)$$

RESULTS AND DISCUSSION

All results are presented in terms of standard nondimensional coefficients and have been corrected for tare-interference effects when such corrections were applicable. Corrections have been applied for the effects of jet-boundary interference on the angle of

attack and on the drag coefficients. No corrections have been made for the effect of the jet boundary on the velocity measured with propellers operating. In view of the large ratio of jet diameter to propeller diameter, however, the jet-boundary effect is believed to be quite small.

The propeller characteristics for a range of blade angles are presented and a brief discussion of the effects of change in airplane attitude and cowling-air flow on these characteristics is given. The effects of variations in cowling exit on the rate of internal flow for conditions with and without the propeller operating as well as the effects of these variations on nacelle drag are also discussed.

Propeller Characteristics

The propulsive efficiency, thrust, and power characteristics measured with the angle of attack of the thrust line at -1° and with the cowling flaps set at 0.5° are presented for a range of blade angles from 20° to 60° in figures 8 to 10.

The envelope propulsive efficiency (fig. 8) rises from a value of approximately 88.5 percent at $\beta = 20^\circ$ to a maximum value of nearly 93 percent at $\beta = 45^\circ$, and then gradually decreases to a value of about 88.5 percent at $\beta = 60^\circ$. Such values of propulsive efficiency are in excess of those normally experienced with more conventional propellers. These values are in good agreement, however, with the values obtained from tests in the NACA 8-foot high-speed tunnel of other propellers incorporating NACA 16-series airfoil sections in the blade design.

The values of efficiency shown in figure 8 are high in comparison with those values obtained from tests of propeller-nacelle combinations, probably because of the fact that: (1) the 16-series airfoil sections, which were incorporated in the design of the blade and which extended well into the blade shank, produced low profile-drag losses; (2) the aerodynamic design of the propeller was such as to produce low axial- and rotational-energy losses; and (3) the presence of the wing in the slipstream reduced the rotational-energy losses.

The breaks in the slopes of the curves of thrust and power against V/nD (figs. 9 and 10) are of interest. These phenomena occur slightly below the stall at all blade angles and become more pronounced at high blade angles. The values of lift coefficient at which the propeller blades operated in the vicinity of the breaks have been determined by the method of reference 4. Comparison of those results with the two-dimensional lift characteristics of the NACA 16-709 airfoil section (reference 5) reveals in both cases pronounced breaks in the lift curves at comparable values of Mach number. Although the breaks occur at a somewhat lower value of lift coefficient in the case of the propeller-blade lift curves than in the case of the lift curve obtained from the two-dimensional airfoil tests, the phenomena are believed to be related.

In order to facilitate the selection of a value of propeller diameter for use in preliminary design calculations, a C_s design chart, based on the results of this investigation, is presented in figure 11. The effects of compressibility are neglected in all design charts of this sort. In view of the fact that these effects are important design considerations, it is essential to take them into account in the selection of propellers for high-speed airplanes.

The results of the propeller tests conducted with the thrust line at 2° and at 5.5° angle of attack and with the cowling flaps set at 0.5°, 11.0°, 15.5°, 20.5°, and 25.5° showed no consistent trends, either with variation of the angle of attack or with cowling-flap deflection. In general, however, the variation in maximum efficiency, from that measured with the thrust line at -1.0° angle of attack and with the cowling flaps neutral, did not in any case exceed $\eta = \pm 0.03$.

Drag and Cowling-Air Flow with Propeller Removed

The effects, on the lift and drag coefficients of the airplane model used in this investigation, of controlling the internal flow through the cowling by cowling flaps and by variable-length cowling skirts are shown in figures 12 and 13, respectively. From the data presented in these figures and from other data based on

measurements of the internal-flow characteristics, the results in figure 14 have been derived. In this figure, comparisons have been made, at values of lift coefficient of 0.1, 0.4, 0.8, and 1.0, of the relative effectiveness of both arrangements as means of controlling the internal flow through the cowling. The effects of cowling flaps and of variable-length cowling skirts on the total nacelle drag coefficient, the drag coefficient due to internal flow, and the parasite-drag coefficient of the nacelle are also compared in the same figure.

It is of particular interest to note from the results presented in figures 12 and 14 that the increment of drag due to cowling-flap deflections of 25° is in certain instances greater than the drag of the entire airplane with cowling flaps retracted. When large cowling-flap deflections are necessary to obtain the pressure drop required for satisfactory engine cooling, the excessive drags due to these deflections will therefore penalize the airplane performance.

Pressure drop through cowling.- From the results of figure 14 the maximum value of cowling pressure coefficient produced by the adjustable cowling flaps is noted to be approximately 1.31; whereas the maximum value of $\Delta p/q_o$ obtained with the variable-length skirt was of the order of 0.75. This difference is, in part, due to the fact that it was not practicable with the particular cowling arrangement investigated to obtain as great an exit area with the variable-length skirts as with the cowling flaps and, in part, due to the fact that the variable-length-skirt arrangement does not produce the low-pressure region at the cowling exit which is obtained by deflecting the cowling flaps.

Effect of internal flow on drag.- For convenience in studying the drag characteristics of the two cowling arrangements, values of the parasite-drag coefficient of the nacelle $C_{D_{n_o}}$ obtained from the faired curves of figure 14 are presented in the following table:

Exit control device	C_L	$C_{D_{n_o}}$		
		$\frac{V_1}{V_o} = 0.45$	$\frac{V_1}{V_o} = 0.50$	$\frac{V_1}{V_o} = 0.55$
Variable-length skirt	0.1	0.075	0.075	0.075
	.4	.075	.067	.060
	.8	.090	.086	.085
	1.0	.107	.100	.098
Cowling flaps	0.1	0.075	0.071	0.067
	.4	.078	.072	.068
	.8	.090	.090	.090
	1.0	.115	.120	.127

At the greatest exit area obtainable with the variable-length skirt, it was not possible to obtain values of the entrance-velocity ratio in excess of 0.57, which is approximately equal to the value obtained with the cowling flaps deflected 5°. From the preceding table it may be noted that, through the range of values of V_1/V_o through which comparisons are possible, the values of $C_{D_{n_o}}$ obtained with both types of control device are nearly equal.

In reference 6, the magnitude of the nacelle parasite-drag coefficient has been shown to be dependent on the ratio of the nacelle diameter to the wing thickness. At a value of this ratio of 0.3, which existed during the present investigation, figure 9 of reference 6 indicates the nacelle drag coefficient $C_{D_{n_o}}$ to be 0.07. This value is in good agreement with the values shown for the low lift range in the preceding table.

At rates of internal flow corresponding to values of V_1/V_o in excess of about 0.65, the results of figure 14 indicate that the profile drag of the nacelle becomes quite large. Such rates of flow required large values of exit area and were obtainable only with large deflections of the cowling flaps. The variation of the

nacelle parasite-drag coefficient with cowling-exit area are compared, at several values of lift coefficient, in figure 15. Correlation of the results given in figure 15 with the data of figure 4 indicate that flap deflections in excess of about 12° create exorbitant increases in drag. It is possible that in this region the cowling flaps start to stall. If such is the case, the high values of drag may be attributed to the resulting poor pressure recovery of the energy in the wake. The values of $C_{D_{n_o}}$ obtained with the large cowling-flap deflections, however, are known to be too great by an indeterminate amount. This fact is explained as follows:

At values of V_1/V_c in excess of 0.65 the pressure drop through the particular cowling arrangement tested is greater than the dynamic pressure of the free stream. Some of the energy required to force the air through the internal passage of the cowling consequently is absorbed from the air flowing over the outside of the nacelle. Under such conditions all the drag chargeable to the internal flow through the nacelle cannot be accounted for from consideration of the loss in momentum of the air flowing through the cowling. The value of C_{D_F} computed from equation (5) is therefore too low by an indeterminate amount and, since $C_{D_{n_o}}$ is defined as the difference between C_{D_n} and C_{D_F}, a low value of C_{D_F} will be reflected as an increase in the parasite-drag coefficient of the nacelle. For this reason the dashed part of the curves of $C_{D_{n_o}}$ against V_1/V_o shown in figure 14 and of $C_{D_{n_o}}$ against K_2 in figure 15 should be interpreted as showing the upper limit of the parasite-drag coefficient of the nacelle rather than its true value.

Effect of Propeller on Flow through Cowling

The values of cowling entrance and exit total-pressure coefficients, obtained at values of β of 20°, 30°, and 40° with various cowling-flap deflections, are shown as a function of V/nD in figure 16. For convenience in making cowling-design estimates, cross plots showing the variation of exit total-pressure coefficient with the exit-area coefficient are presented

in figure 17. Because knowledge of the static pressure at the cowling exit is often of interest, the exit static-pressure coefficients for the same range of values of β and cowling-flap deflection used in figure 16 are presented in figure 18.

The contribution of the propeller to the total pressure at the cowling entrance was found to be essentially independent of the cowling-exit condition. With the propeller operating at low values of V/nD - that is, at high values of thrust loading - the pressure at the cowling entrance is increased. The effect diminishes with increasing values of V/nD - that is, with decreasing values of thrust loading. In general, with the particular propeller-cowling arrangement tested, the effect of the propeller appears to be negligible at values of the thrust-loading coefficient of less than about $T_C = 0.1$.

The distribution of the total pressure of the air entering the cowling is of concern in considerations of engine-cooling characteristics. Because of numerous pecularities of the flow, this pressure is seldom uniform. It depends, among other things, on the operating condition of the propeller and on the attitude of the airplane.

The manner in which the differences in top and bottom cowling-entrance pressure, measured with the propeller removed, are influenced by angle of attack is shown in figure 19. At small deflections of the cowling flap, the pressure at the top of the cowling decreases rapidly with increase in angle of attack. At very large openings of the cowling flap, the top and bottom pressures tend to remain more nearly uniform throughout the angle-of-attack range. It is probable that, at the low rates of internal flow encountered with small deflections of the cowling flaps, considerable spillage occurred at the cowling entrance. The increased entrance velocity obtained by opening the cowling flaps tended to create a more stable condition of flow and thereby to promote a more nearly uniform distribution of pressure over the cowling entrance.

The effect of the propeller on the front-pressure variation may be observed from comparison of the results in figure 19 with the results presented in figure 20. The propeller operating in front of the cowling increased the average pressure over the entire cowling entrance

(fig. 16) and, except at the smallest deflection of the cowling flaps at which the low entrance velocity allows for unstable flow conditions, also tended to equalize the distribution of pressure over the cowling entrance.

The variation of the pressure at the cowling exit with V/nD is dependent on the cowling-exit condition (figs. 16, 17, and 18). With large deflections of the cowling flaps, the low pressure coefficients at the cowling exit, obtained with the propeller operating, were accentuated at low values of V/nD. As the values of V/nD were increased, these pressure coefficients tended to approach those obtained with the propellers removed. With small deflections of the cowling flaps, the exit pressure tended to become greater than that of the free stream at low values of V/nD. This effect is probably due to the fact that, at small flap deflections, the exit area was reduced to such extent that the air inside the cowling was compressed by the action of the propeller on the flow at the cowling entrance.

The effect of the propeller operating at low values of V/nD in conjunction with large cowling-flap deflections was such as to produce high rates of flow thrcugh the nacelle. It is therefore indicated that a powerful means will be provided for obtaining adequate engine cooling for ground operation and take-off.

Influence of Cooling Requirements on Airplane Performance

In the case of many conventional radial air-cooled engine installations, the pressure drop required to produce sufficient cooling-air flow can be obtained only when the cowling flaps are extended to large deflections. The drag produced by such large flap deflections often causes a substantial decrease in airplane performance.

This consideration suggests the possibility of achieving improved airplane performance through the adoption of a cooling arrangement that is not penalized by the large momentum and pressure losses which are inherent in the conventional engine-cooling system. One such plan, which has frequently been proposed, would incorporate in the cooling system a blower of such capacity that the energy added to the cooling air by the blower would just suffice to overcome the internal losses of the system. With such a device the cooling-air

passages could be arranged to allow the cooling air to be exhausted at free-stream velocity, thereby eliminating the wake-momentum losses. In addition, the detrimental drag losses associated with large deflections of the exit flap would be eliminated.

The advantages attainable through the adoption of the blower-cooling system cited previously are best illustrated by comparing the performances of an airplane that achieves engine cooling in one case through the use of a conventional engine-cooling system and in another case through the use of an auxiliary blower.

Consider, for example, the performance of a twin-engine military airplane operating at an altitude of 14,000 feet and having the following assumed characteristics:

Engines, P. & W. R-2800 with single-stage two-speed geared supercharger	
Engine cruise rating	1200 brake horsepower at 2100 rpm
Propeller diameter, feet	12.5
Propeller gear ratio	2:1
Wing area, square feet	540
Gross weight, pounds	25,000
Maximum cross-sectional area of nacelle, square feet	17.5
Altitude, feet	14,000
Fuel-air ratio for cruise	0.07
Maximum temperature, rear spark-plug gasket, $^{\circ}F$	400

From the data presented in figures 8 to 10, the operating conditions of the propeller are readily determined. Figure 21 shows the variation of V/nD, η, and β with airspeed. For convenience, calculations are presented for a true airspeed of 260 miles per hour. Correlation of the propeller-operating characteristics with the engine-power rating and speed of flight yield the following:

$$V/nD = 1.744$$

$$\beta = 45.1^{\circ}$$

$$\eta = 0.856$$

$$\text{Horsepower available} = \eta P$$

$$= 2054 \text{ horsepower (two engines)}$$

In determining the power required, it will be assumed that the geometry of the example airplane is similar to that of the model used in this investigation. The lift and drag characteristics of figure 12 are therefore applicable. These results, however, do not include the drag effects chargeable to such items as armament, oil cooler, radio antenna, and manufacturing irregularities. It will therefore be assumed that an incremental drag coefficient of $\Delta C_D = 0.0035$ will account for these additional drag items. On this basis, for a wing loading of 46.3 pounds per square foot and an airspeed of 260 miles per hour, the lift and drag coefficients of the airplane without nacelles are found to be as follows:

$$C_{D'} = C_D + \Delta C_D$$

$$= 0.0191 + 0.0035$$

$$= 0.0226 \text{ (at } C_L = 0.412)$$

The drag chargeable to the power-plant installation consists of its parasite drag plus the drag resulting from the change in momentum of the air passing through the cooling system. In making precise design calculations of the magnitude of the drag due to momentum changes, it is important that heating and compressibility effects be accounted for. These effects are discussed in reference 7. In order to achieve simplicity in the present example, however, these effects will be neglected. The values derived in the ensuing calculations must therefore be considered as merely indicative of the true drag.

Evaluation of the drag chargeable to the conventional engine-cooling system will require different treatment from that required for the blower-cooling system. The following section will therefore deal separately with the two cases. In each case the cowling will be equipped with flaps.

Case I - Conventional engine-cooling system.- By correlation of the assumed values for the airplane characteristics with results of cooling tests of the example engine, the variation of the required total- to

static-pressure drop across the engine ΔH with airspeed has been determined and is shown in figure 22. The static and total pressures at the rear of the engine are assumed to be equal. The total- to static-pressure drop may therefore be treated as a change in total pressure. For an airspeed of 260 miles per hour, it is found that $\Delta H/q_o$ is 0.919 with a corresponding air flow of 811.9 cubic feet per second, which remains essentially constant at airspeeds ranging from 220 to 320 miles per hour. It is assumed that losses $\Delta H/q_o$ in the diffuser and in the exit are 0.15 and 0.05, respectively; therefore, the loss of total pressure through the cowling $\frac{H_1 - H_2}{q_o}$ is 1.119. At the flight condition under consideration ($V/nD = 1.744$, $\beta = 45.1^\circ$, and $C_L = 0.412$), the front-pressure coefficient is found, from figure 16, to be $\frac{H_1 - H_o}{q_o} = -0.073$. In order to provide the required rate of flow, the total-pressure coefficient at the exit must be

$$\frac{H_o - H_2}{q_o} = \frac{H_1 - H_2}{q_o} - \frac{H_1 - H_o}{q_o}$$

$$= 1.119 - (-0.073)$$

$$= 1.192$$

By making the simplifying assumption $\rho_o = \rho_1 = \rho_2$ and transforming the internal drag defined in equation (3) to a coefficient form, the increment of drag coefficient due to the air flow through one nacelle may be expressed in terms of variables that are now known as

$$\Delta C_{D_F} = \frac{2Q}{SV_o}\left[\sqrt{1 + \frac{H_1 - H_o}{q_o}} - \sqrt{1 - \frac{H_o - H_2}{q_o}}\right]$$

$$= \frac{2 \times 811.9}{540 \times 260 \times \frac{88}{60}}\left[\sqrt{1 + (-0.073)} - \sqrt{1 - 1.192}\right] \quad (13)$$

The term $\sqrt{1 - \frac{H_o - H_2}{q_o}}$ describes the final wake velocity of the air passing through the cowling. For the particular case under consideration, this term does not yield a real value. The calculation may therefore be completed by assuming that the final wake velocity is zero, and the additional power required for cooling will be charged to the parasite drag of the nacelle. The increment of drag coefficient then becomes

$$\Delta C_{D_F} = \frac{2 \times 811.9}{540 \times 260 \times \frac{88}{60}} \sqrt{1 + (-0.073)}$$

$$= 0.0076$$

It is now desired to determine the effect of the parasite resistance of the nacelle. By interpolating the results of figure 17, it is found that, at the flight condition under consideration ($V/nD = 1.744$, $\beta = 45.1^\circ$, and $C_L = 0.412$), a value of exit-area-ratio coefficient of $K_2 = 0.390$ is necessary to produce the required value of $\frac{H_o - H_2}{q_o}$ of 1.192. From figure 4 it is seen that a cowling-flap deflection of 18° is needed. (Fig. 23 shows the variation of cowling-flap deflection with airspeed for the example airplane.) By applying the results of figure 15 and taking into account the value of lift coefficient at which the airplane is operating, the value of nacelle-parasite-drag coefficient is found to be $C_{D_{n_o}} = 0.158$. On the basis of wing area, the increment of parasite-drag coefficient chargeable to one nacelle is

$$\Delta C_{D_n} = \frac{A_n}{S} C_{D_{n_o}}$$

$$= \frac{17.5}{540} \times 0.158$$

$$= 0.0051$$

The total-drag coefficient for the complete airplane is

$$C_D = C_{D'} + 2\Delta C_{D_F} + 2\Delta C_{D_n}$$

$$= 0.0226 + 0.0152 + 0.0102$$

$$= 0.0480$$

The power required for level flight at V = 260 miles per hour is

$$\frac{C_D q_o S V_o}{550} = \frac{0.0480 \times 112.3 \times 540 \times 260 \times \frac{88}{60}}{550}$$

$$= 2022 \text{ horsepower}$$

Case II - Blower-cooling system.- It is assumed that the energy added to the air by the blower will just suffice to overcome the internal losses. In this case, the power input to the blower is represented by the following equation

$$\text{Blower power} = \frac{Q(H_1 - H_2)}{\eta_B}$$

where η_B is the blower efficiency and will be assumed to have the value of 0.80 for this example.

The energy supplied to the blower may be expressed in terms of equivalent increment of airplane-drag coefficient

$$\Delta C_{D_B} = \frac{811.9 \times 1.119}{0.80 \times 260 \times \frac{88}{60} \times 540}$$

$$= 0.0054$$

When the velocity of the air at the cowling exit is equal to that of the free stream, the cowling-exit-area ratio is

$$K_2 = \frac{Q}{A_n V_o}$$

$$= \frac{811.9}{17.5 \times 260 \times \frac{88}{60}}$$

$$= 0.122$$

From figure 15 the corresponding value of $C_{D_{n_o}}$ is 0.079 for a value of $C_L = 0.412$. The increment of drag coefficient chargeable to the parasite resistance of the nacelle is

$$\Delta C_{D_n} = C_{D_{n_o}} \frac{A_n}{S}$$

$$= 0.0780 \times \frac{17.5}{540}$$

$$= 0.0025$$

The total-drag coefficient of the complete airplane is

$$C_D = C_D' + 2\Delta C_{D_B} + 2\Delta C_{D_n}$$

$$= 0.0226 + 0.0108 + 0.0050$$

$$= 0.0384$$

The power required for level flight at V = 260 miles per hour is

$$\frac{C_D q_o S V_o}{550} = \frac{0.0384 \times 112.3 \times 540 \times 260 \times \frac{88}{60}}{550}$$

$$= 1613 \text{ horsepower}$$

By similar calculations, the performance characteristics for other speeds may be determined. The results of such calculations are shown in figure 24. These results indicate that the example airplane can cruise at approximately 311 miles per hour with the blower-cooling system; whereas the maximum level-flight cruising speed attainable with the conventional engine-cooling system is approximately 289 miles per hour. By adoption of the blower-cooling system, designed to emit the cooling air at free-stream velocity, an increase in cruising speed of about 22 miles per hour can therefore be obtained over that attained with the conventional engine-cooling system. The values cited are optimistic because some of the gain would be offset by the weight and complexity of the blower installation.

In general, selection of the optimum cooling system for an aircraft power-plant installation involves numerous considerations. The specific design of any installation must be determined from considerations of the special problems that each particular airplane presents. An engine for which the cooling system is designed for low-altitude operation may not be able to cool at high altitudes without the penalty of greatly increased drag power losses brought about by the large cowling-flap deflections required. In some cases considerable reduction of the drag power losses can be realized through the use of a blower in the cooling system. Such drag reduction may be reflected in either greater cruising speed, improved performance in climb, increased range, or in high-altitude operation.

CONCLUSIONS

1. The maximum values of propulsive efficiency measured in this investigation varied from 88 percent at a value of V/nD of 0.8 to nearly 93 percent at a value of V/nD of 2.4 and then gradually decreased to about 89 percent at a value of V/nD of 3.8.

2. In the range of flow attainable with a variable-length cowling skirt, the parasite drag of the nacelle, when equipped with this arrangement, was approximately the same as when it was fitted with adjustable cowling flaps and in either case was not excessive.

3. The parasite drag of nacelles equipped with cowling flaps of approximately the same proportions of those investigated is moderate and does not increase appreciably with cowling-flap deflections of 12° or less. Values of pressure drop required for satisfactory engine cooling may be obtained by deflecting the cowling flaps to angles in excess of 12° at the expense of rapidly increasing the drag. This increase of drag may reach such magnitude as to double the drag of the entire airplane.

4. For ground cooling and take-off, it is indicated that well-designed cowling flaps, extended to large deflections, provide a powerful means for obtaining adequate air flow for engine cooling. Such air flow is not attainable from nacelles equipped with variable-length cowling skirts.

Langley Memorial Aeronautical Laboratory
National Advisory Committee for Aeronautics
Langley Field, Va.

REFERENCES

1. McHugh, James G., and Derring, Eldridge H.: The Effect of Nacelle-Propeller Diameter Ratio on Body Interference and on Propeller and Cooling Characteristics. NACA Rep. No. 680, 1939.

2. Valentine, E. Floyd: Preliminary Investigation Directed toward Improvement of the NACA Cowling. NACA ARR, April 1942.

3. Theodorsen, Theodore, Brevoort, M. J., and Stickle, George W.: Full-Scale Tests of N.A.C.A. Cowlings. NACA Rep. No. 592, 1937.

4. Lock, C. N. H.: A Graphical Method of Calculating the Performance of an Airscrew. R. & M. No. 1849, British A.R.C., 1938.

5. Stack, John: Tests of Airfoils Designed to Delay the Compressibility Burble. NACA TN No. 976, Dec. 1944. (Reprint of ACR, June 1939.)

6. McHugh, James G.: Tests of Several Model Nacelle-Propeller Arrangements in Front of a Wing. NACA ACR, Sept. 1939.

7. Becker, John V., and Baals, Donald D.: The Aerodynamic Effects of Heat and Compressibility in the Internal Flow System of Aircraft. NACA ACR, Sept. 1942.

TABLE I.- TESTS WITH PROPELLER OPERATING

[All angles given in deg]

Cowling-flap angle, β	Angle of attack					
	0.5	5.5	11.0	15.5	20.5	25.5
20	-1	-1	-1	-1	-1	-1
	2	2	2	2	2	2
	5.5	------	------	5.5	5.5	5.5
25	-1	------	------	------	------	------
30	-1	-1	-1	-1	-1	-1
	2	2	2	2	2	2
	5.5	5.5	5.5	5.5	5.5	5.5
35	-1	------	------	------	------	------
40	-1	-1	-1	-1	------	------
	2	2	2	2	------	------
	5.5	------	------	5.5	------	------
45	-1	------	------	------	------	------
50	-1	------	------	------	------	------
	2	------	------	------	------	------
55	-1	------	------	------	------	------
60	-1	------	------	------	------	------

TABLE II.- TESTS WITH PROPELLER REMOVED

[All angles given in deg; lengths given in in.]

α	Cowling arrangement
-1 to 8	Cowling-flap angles of 0.5, 5.5, 11.0, 15.5, 20.5, 25.5
-1 to 8	Cowling-flap lengths of 3.25, 2.75, 2.25, 1.75, 1.25
-1 to 8	Nacelles removed

L-638

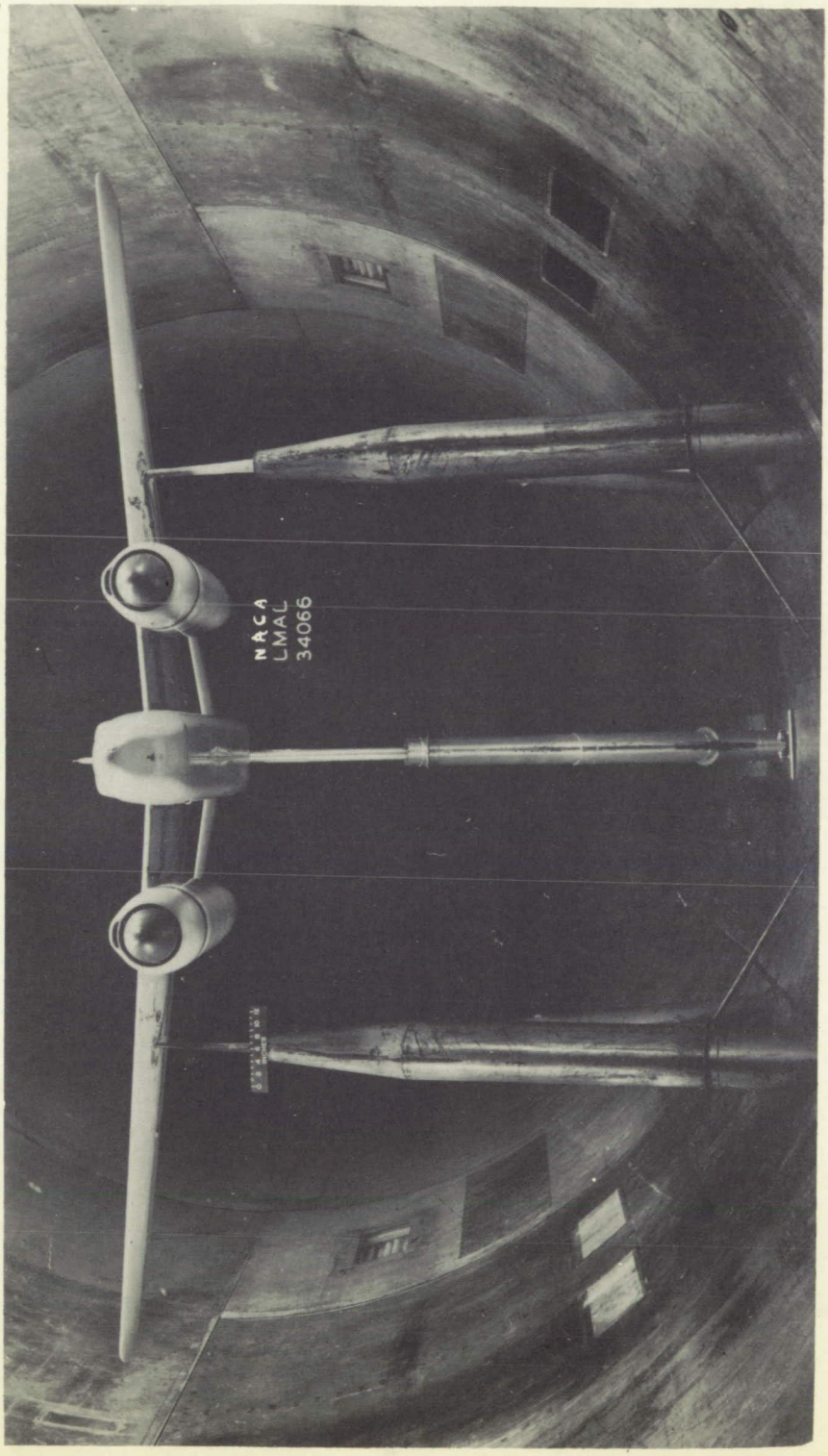

Figure 1.- Installation of airplane model in NACA 19-foot pressure tunnel.

L-638

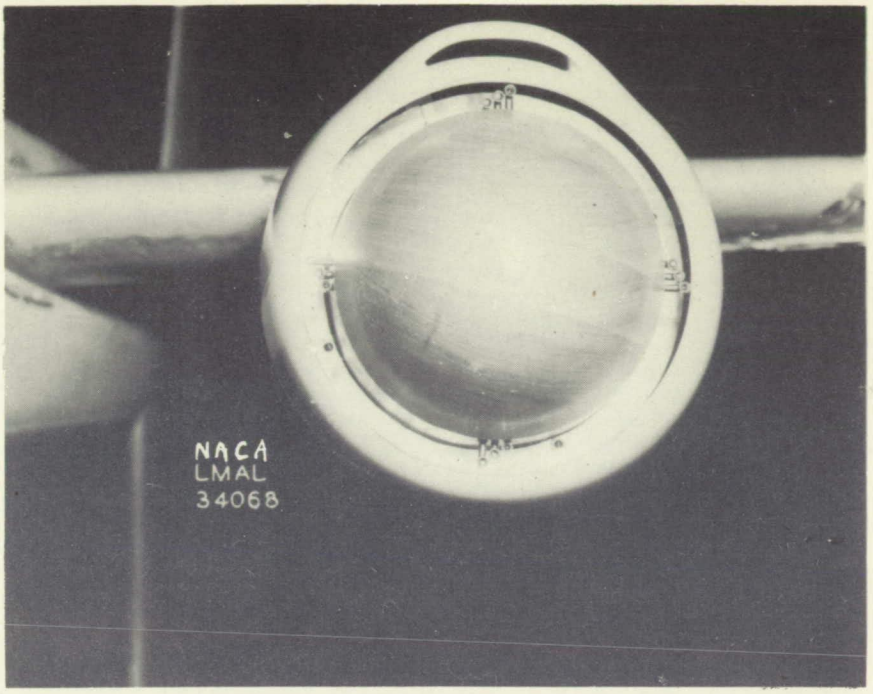

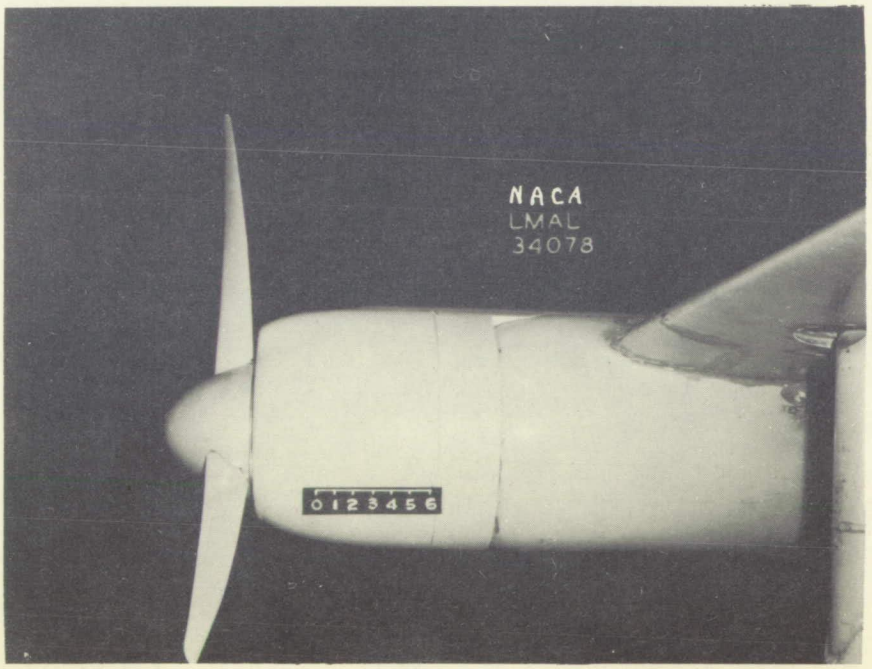

Figure 2.- General arrangement of nacelle.

L-638

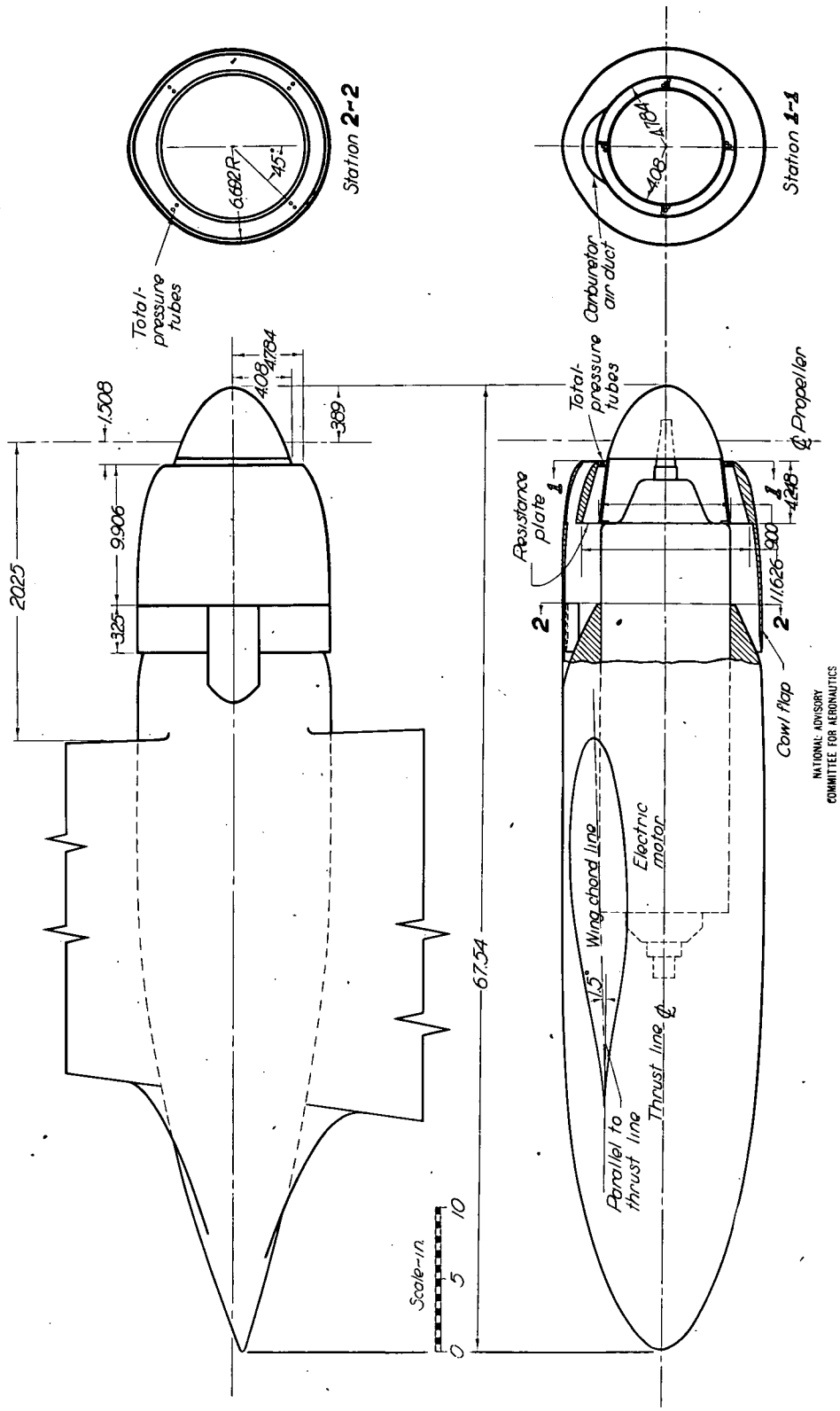

Figure 3.- Details of nacelle.

L-638

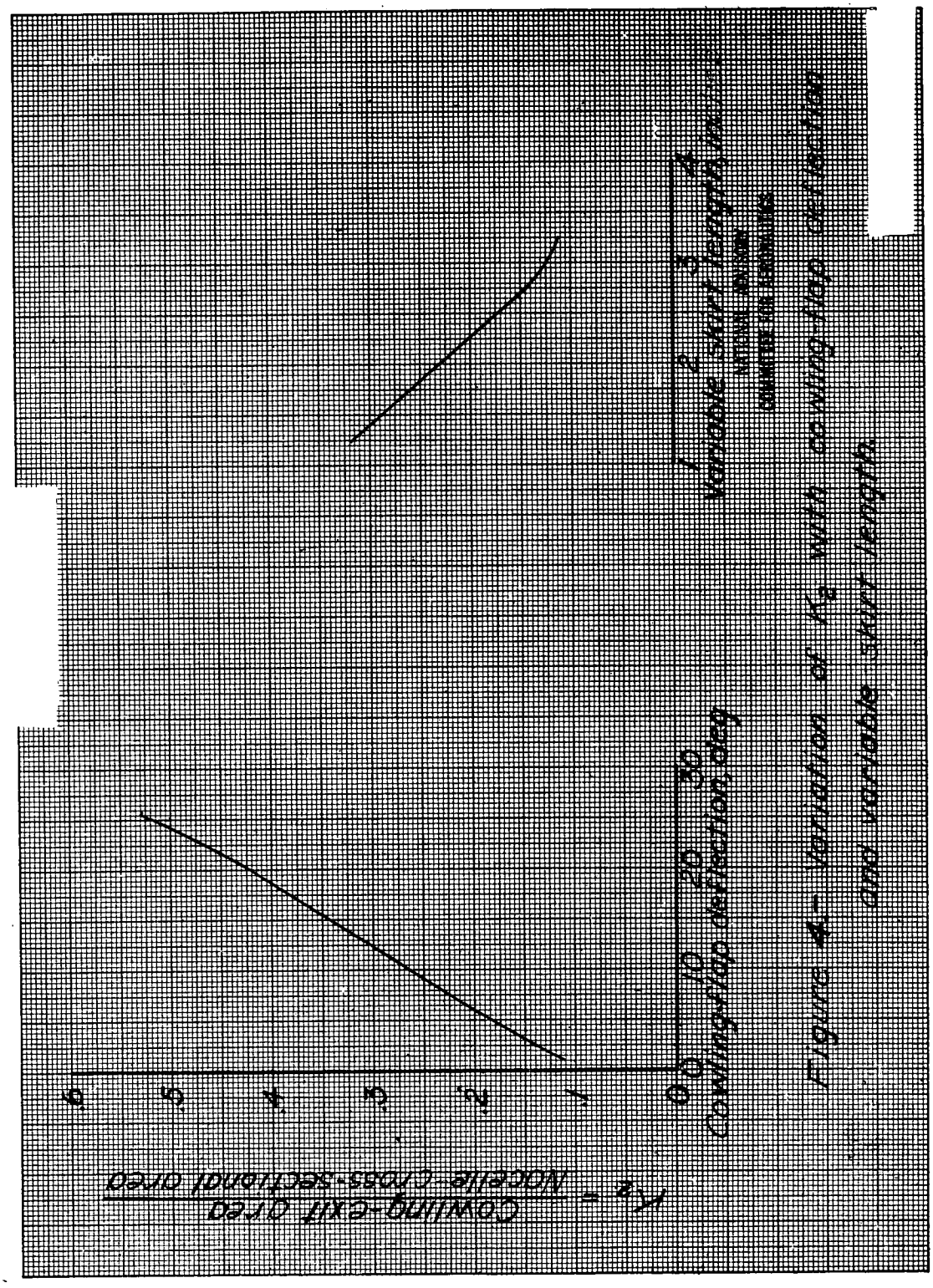
Figure 4.- Variation of K_2 with compression ratio for various values of ramp-exit throat Mach number.
Compression ratio, p_0/p_∞
Boundary-layer correction, $K_2 = \frac{\text{Combustor-exit area}}{\text{Nozzle-throat cross-sectional area}}$
0
.5
1.0
1.5
2.0
2.5
3.0

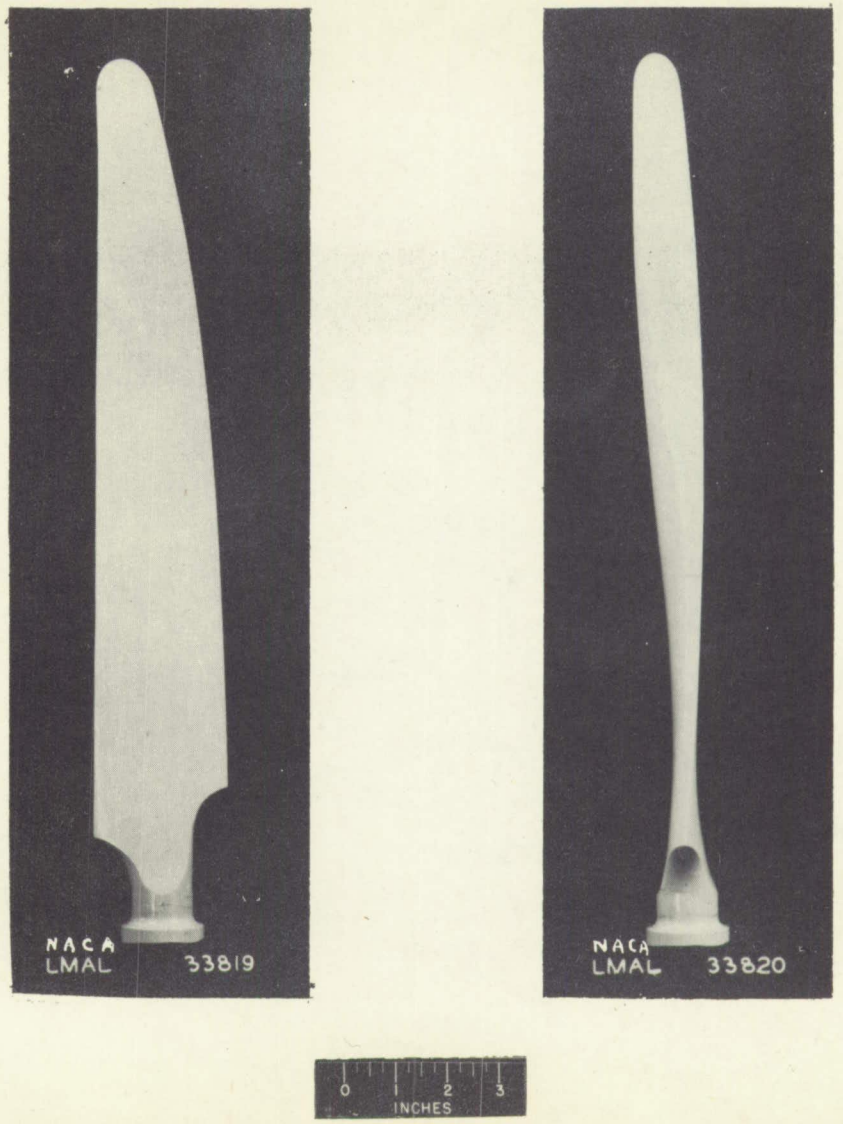

Figure 5.- Details of Hamilton Standard 6457A-6 model propeller blade.

L-638

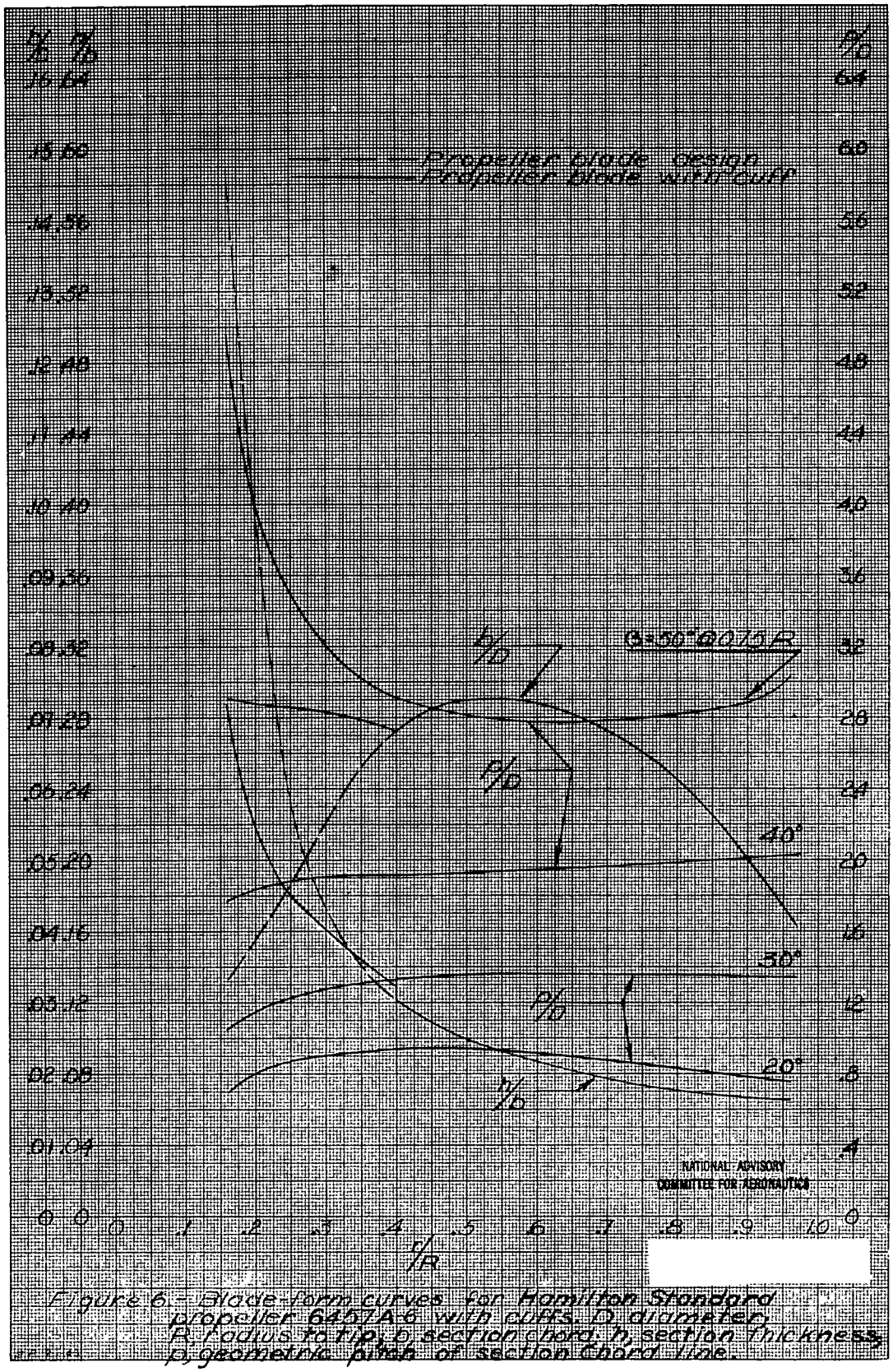

Figure 6.- Blade-form curves for Hamilton Standard propeller 6457A-6 with cuffs. D, diameter; R, radius to tip; b, section chord; h, section thickness; β, geometric pitch of section chord line.

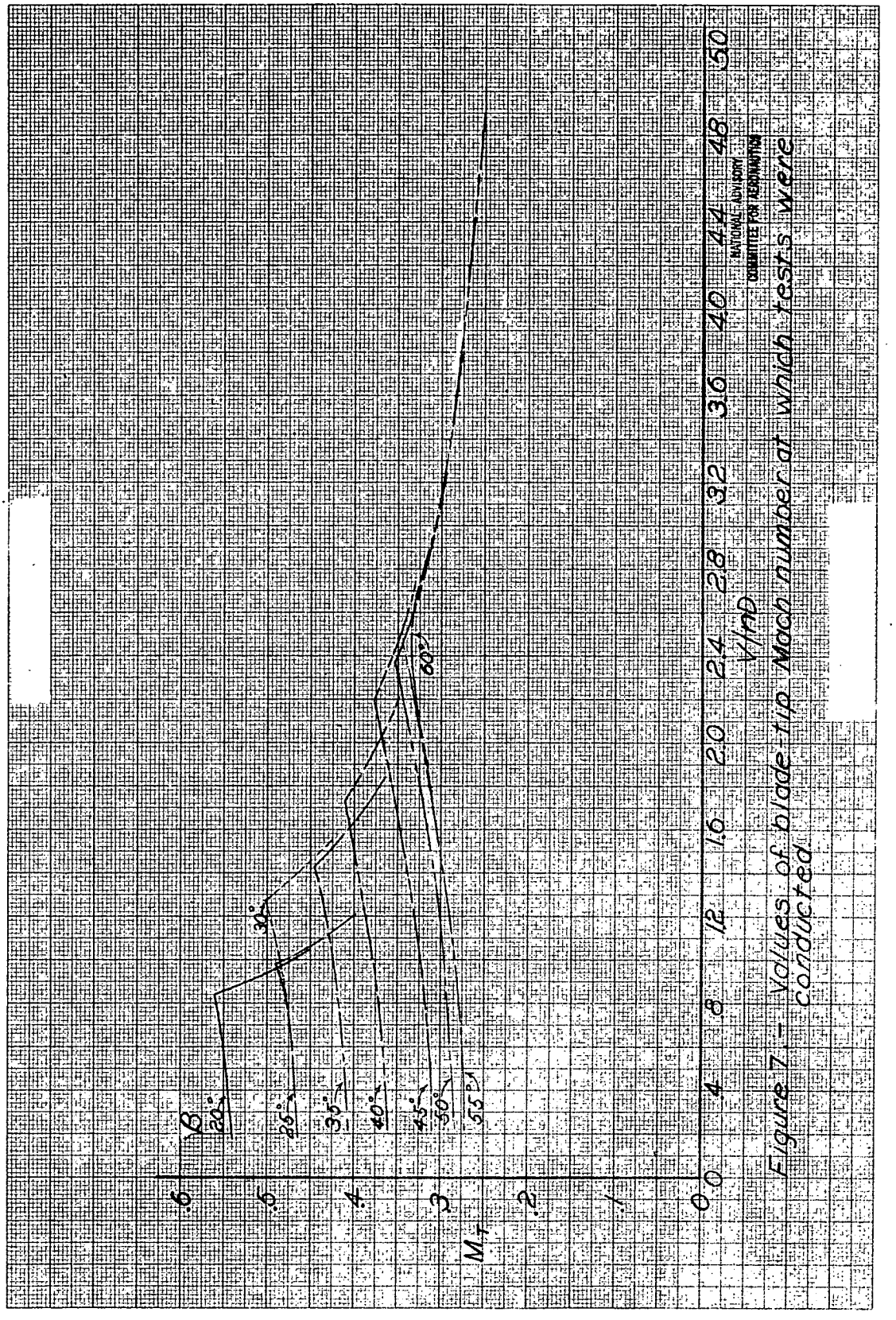

Figure 7.- Values of blade tip Mach number at which tests were conducted.

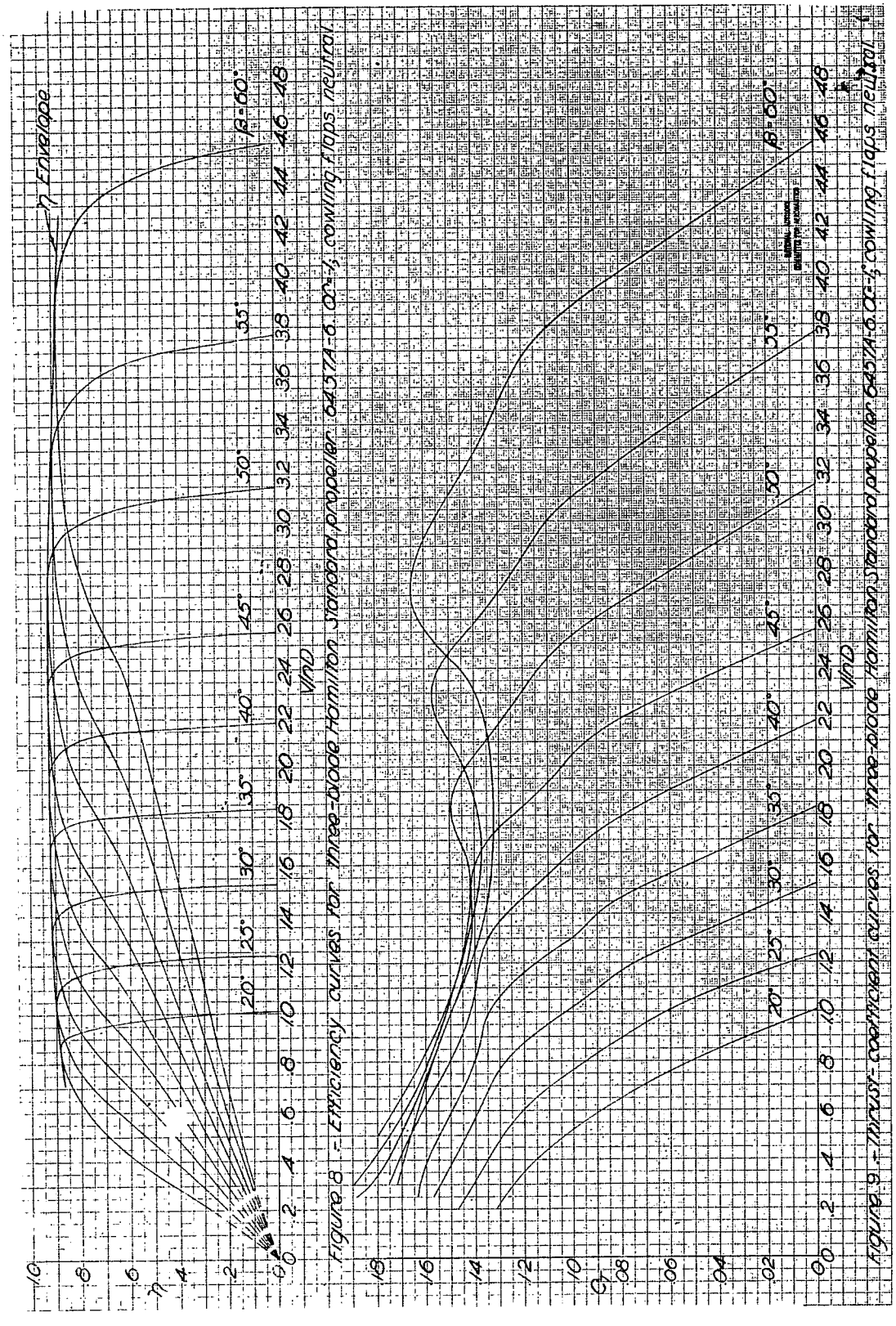

Figure 8 - Efficiency curves for three-blade Hamilton Standard propeller 6457A-6 on XP-47B airplane.

Figure 9 - Thrust coefficient for three-blade Hamilton Standard propeller 6457A-6 on XP-47B airplane.

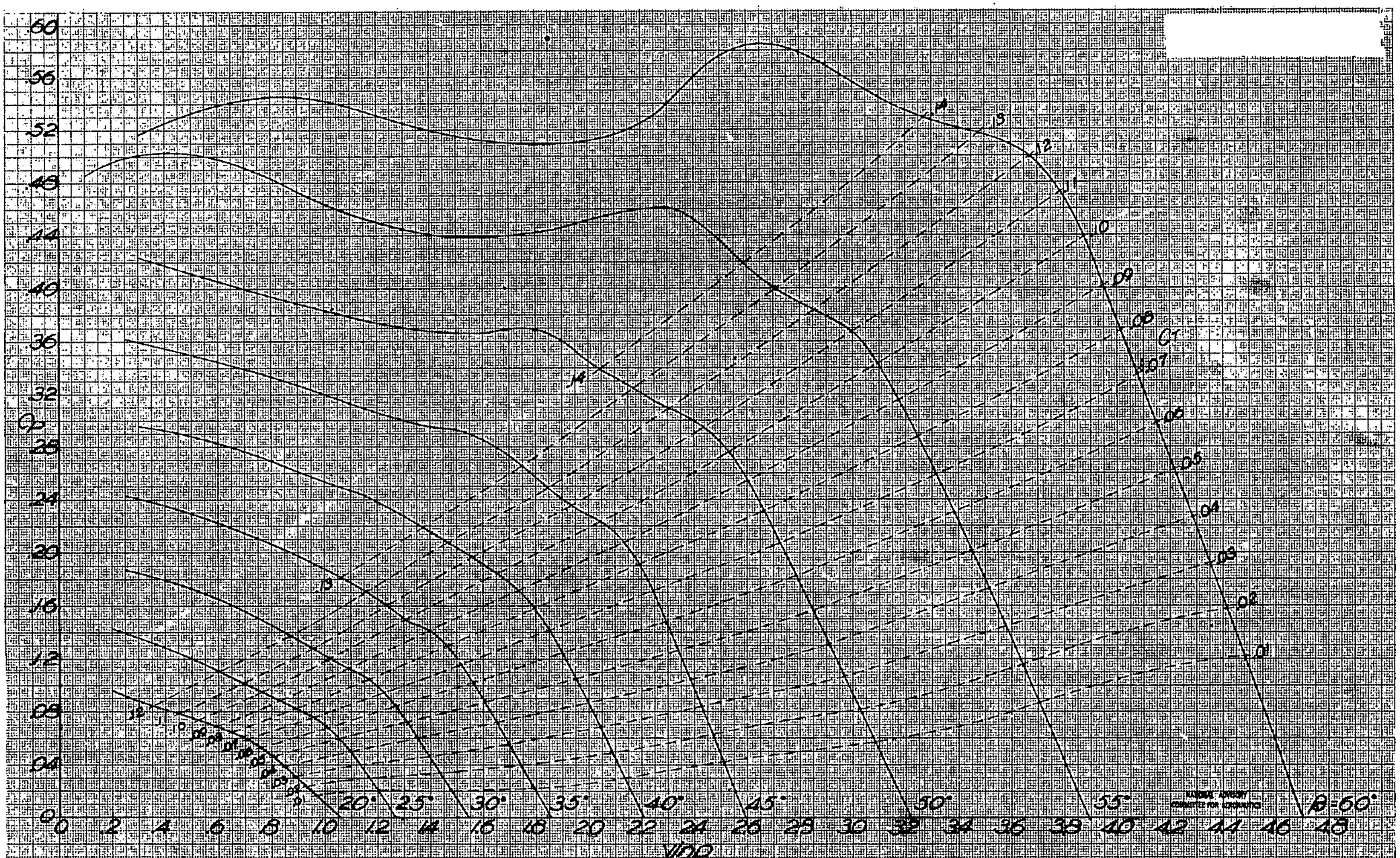

Figure 10.- Power-coefficient curves for three-blade Hamilton Standard propeller 6487A-6. OC-5 cowling flaps neutral.

L-638

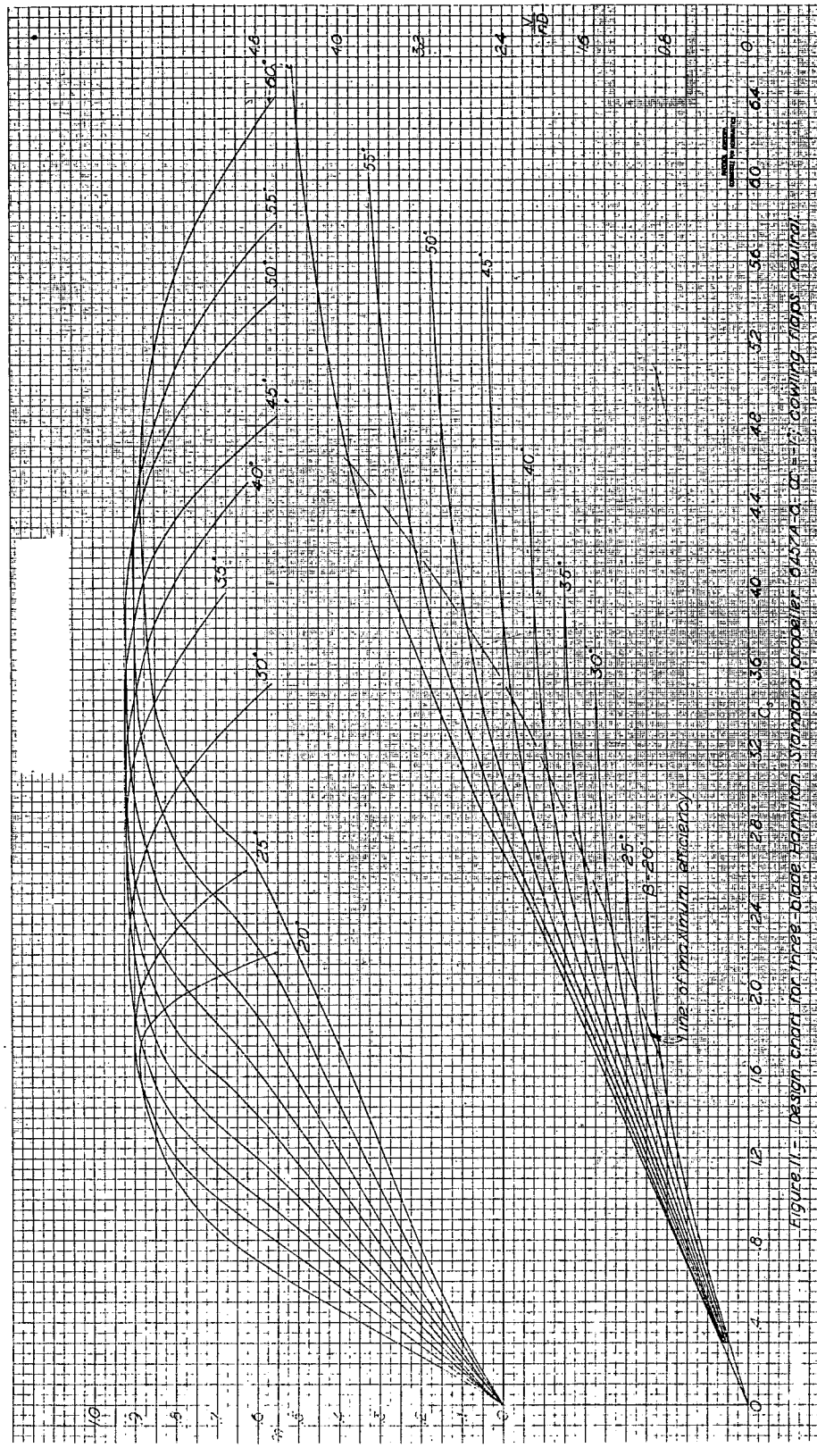
Figure 11.- Design curves for single-slotted flaps. Chord ratio, 0.25; radius ratio, 0.0625.
Curves of maximum section lift coefficient
Flap deflection, δf, deg
Flap-chord ratio, cf/c

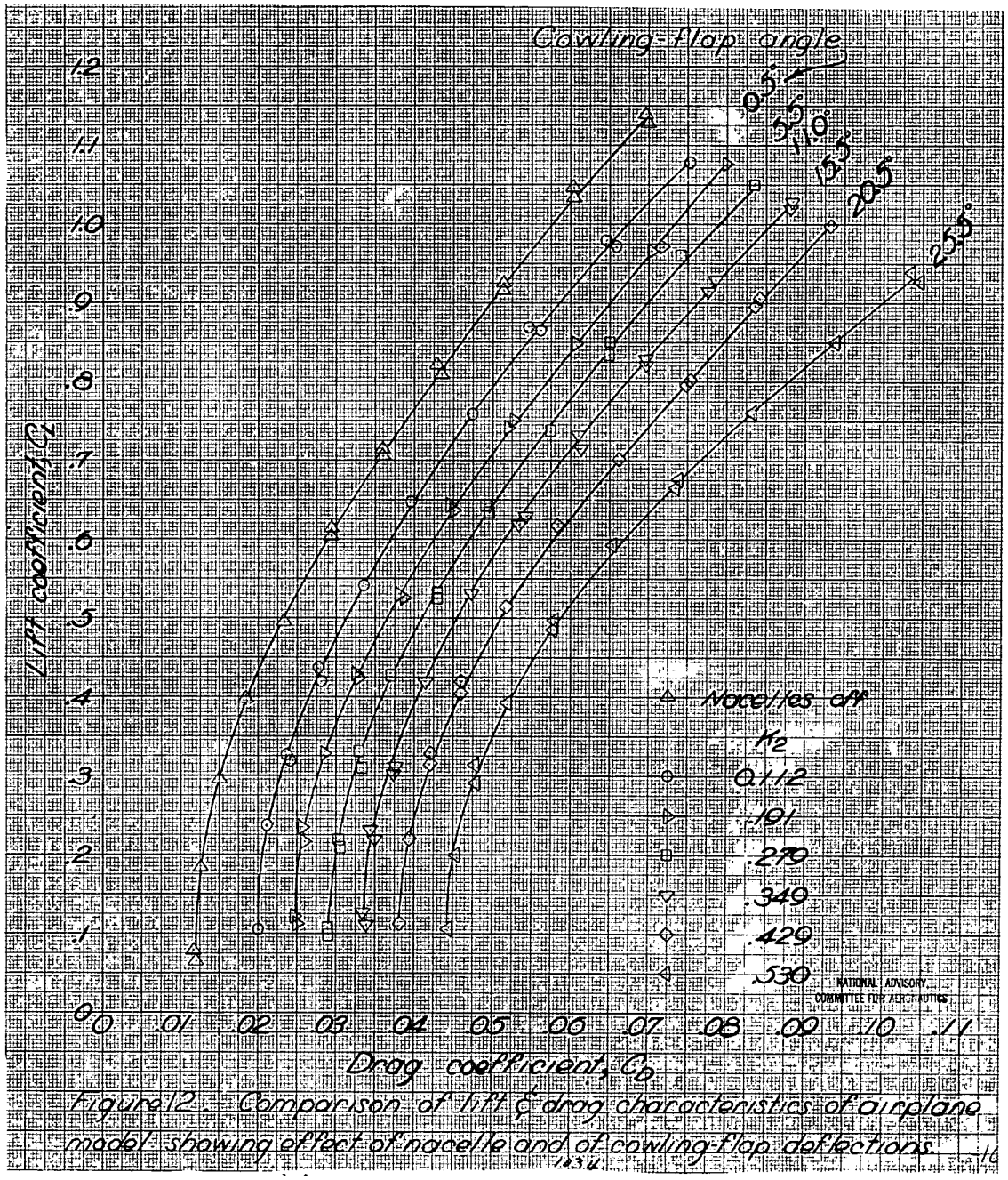

Figure 12.- Comparison of lift and drag characteristics of airplane model showing effect of nacelle and of cowling-flap deflections.

L-638

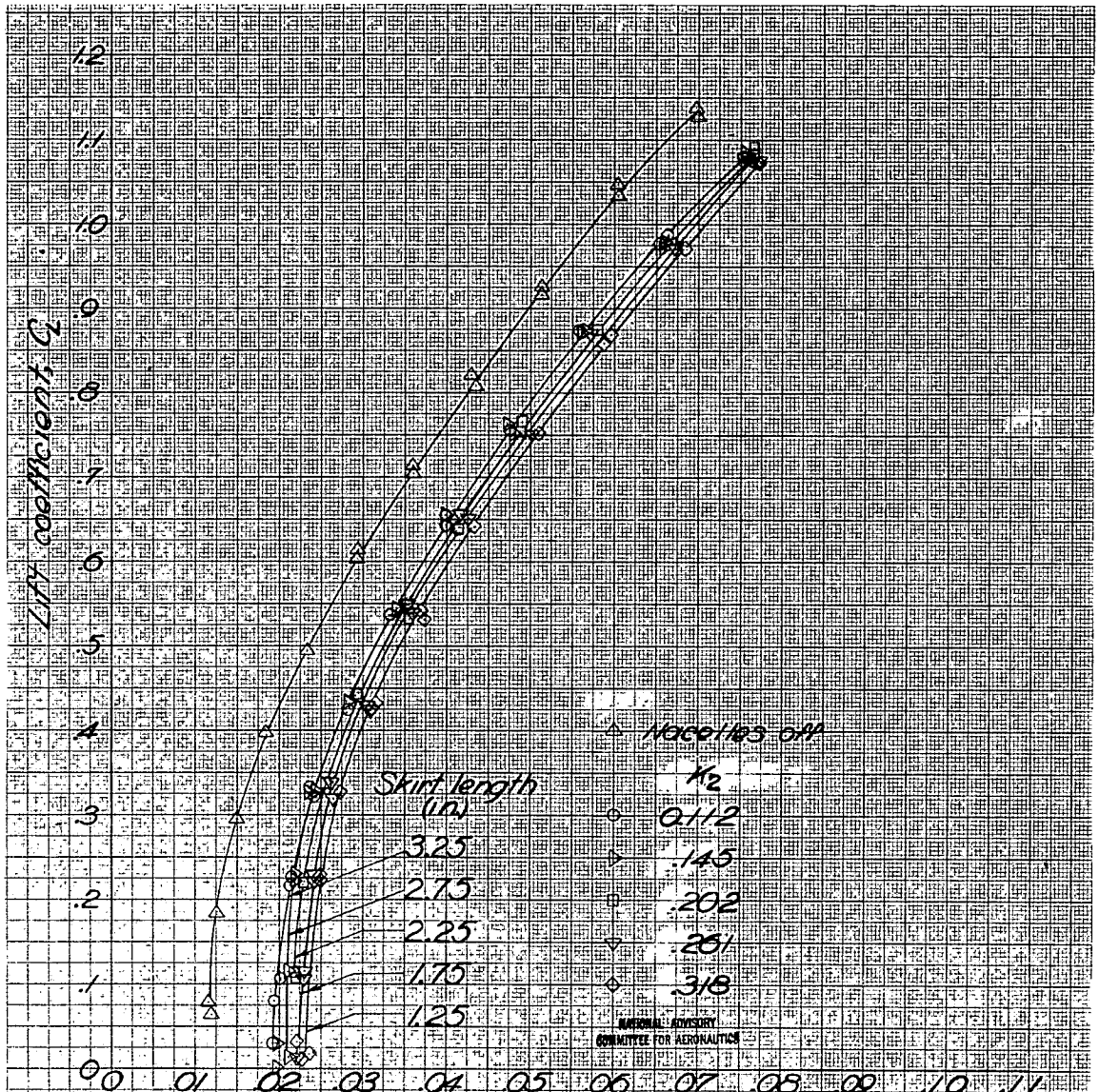

Figure 13.- Comparison of lift & drag characteristics of airplane model showing effect of nacelle and of cowling-skirt length.

L-638

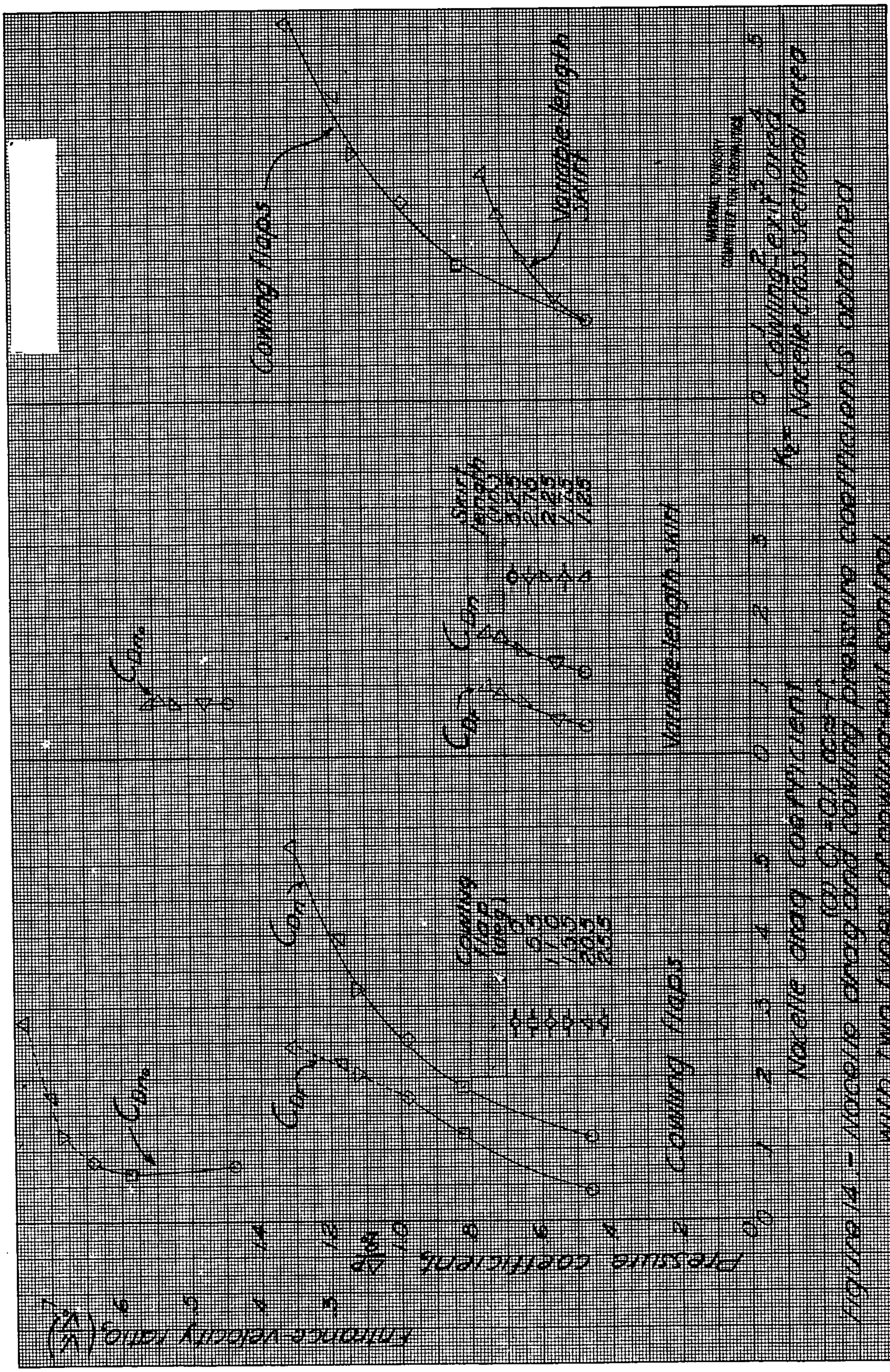

(a) $C_L = 0.1$; $\alpha \approx 1°$.

Figure 14.- Nacelle drag and cowling pressure coefficients obtained with two types of cowling-exit control.

L-638

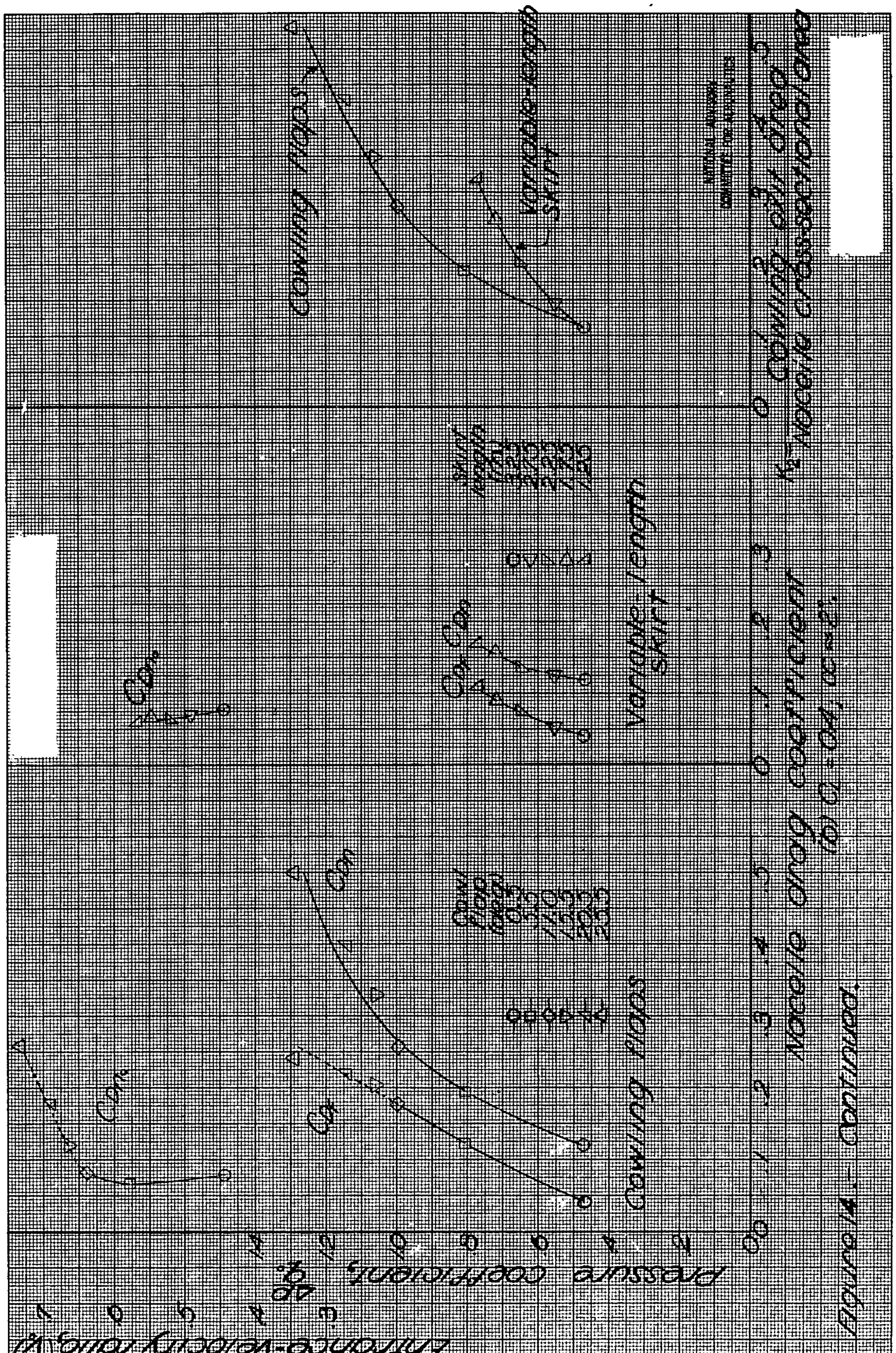

Figure 14.- Continued.

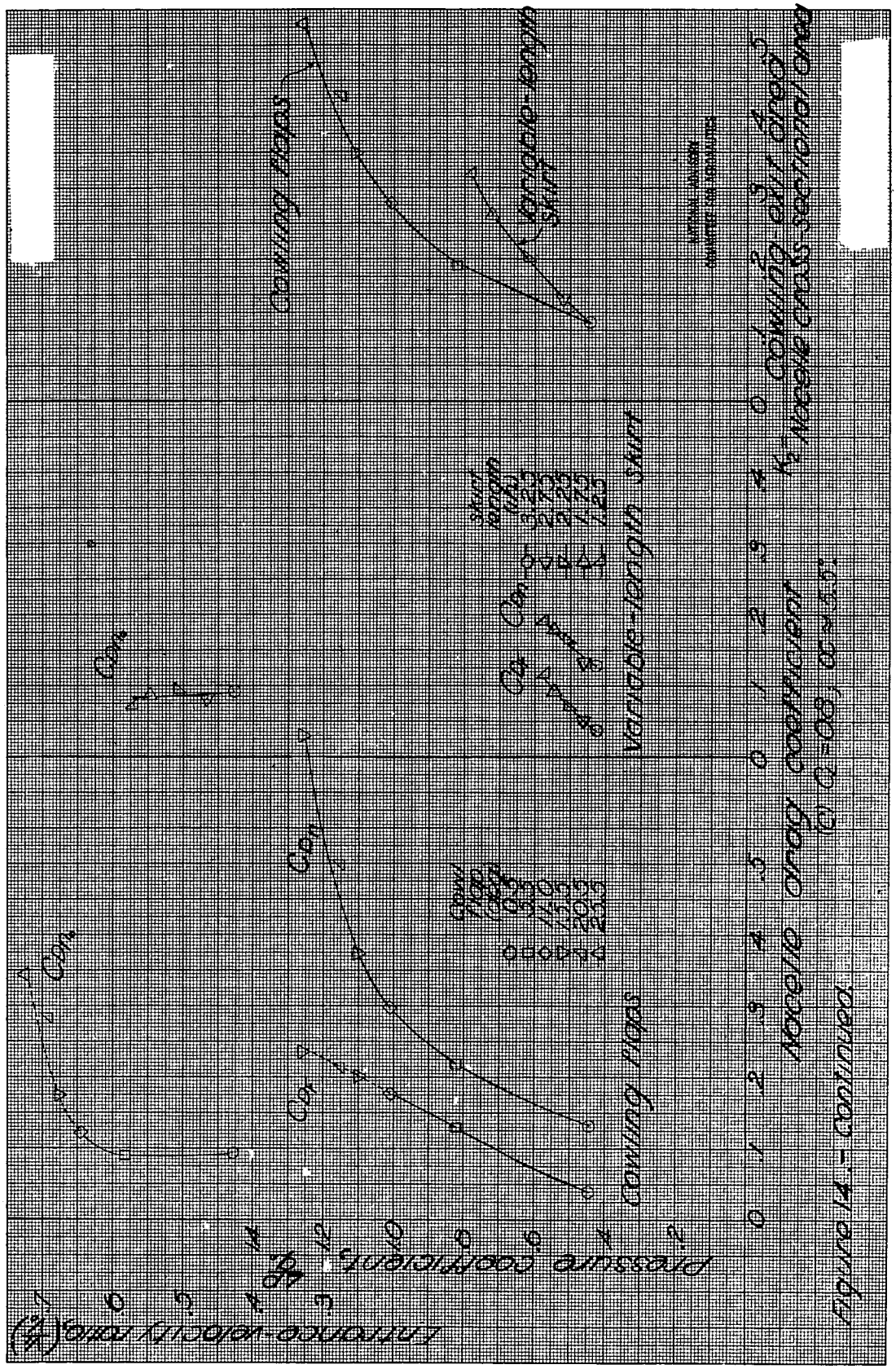
Variable-area exit nozzle
Pressure coefficients, $\frac{p-p_0}{q_0}$
Free-stream Mach number, M_0
Free-stream velocity ratio, $\frac{V_0}{a_0}$
Nozzle area ratio, $\frac{A_e}{A_t}$
Nozzle pressure ratio, $\frac{p_e}{p_0}$
Jet-total-pressure ratio, $\frac{p_j}{p_0}$
Common legend
Continued

L-638

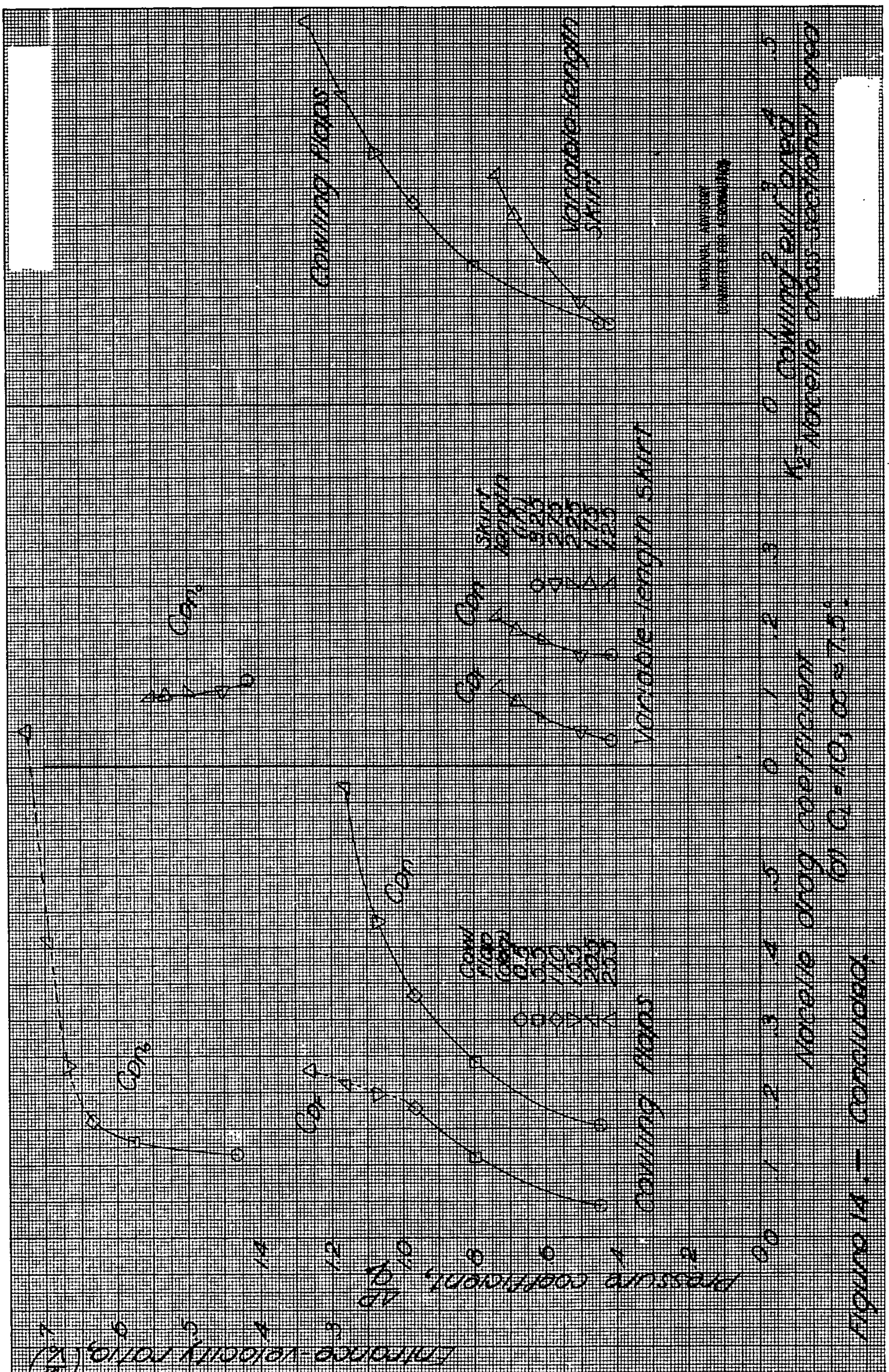

(d) $C_L = 1.0$; $\alpha = 7.5°$.

Figure 14.— Concluded.

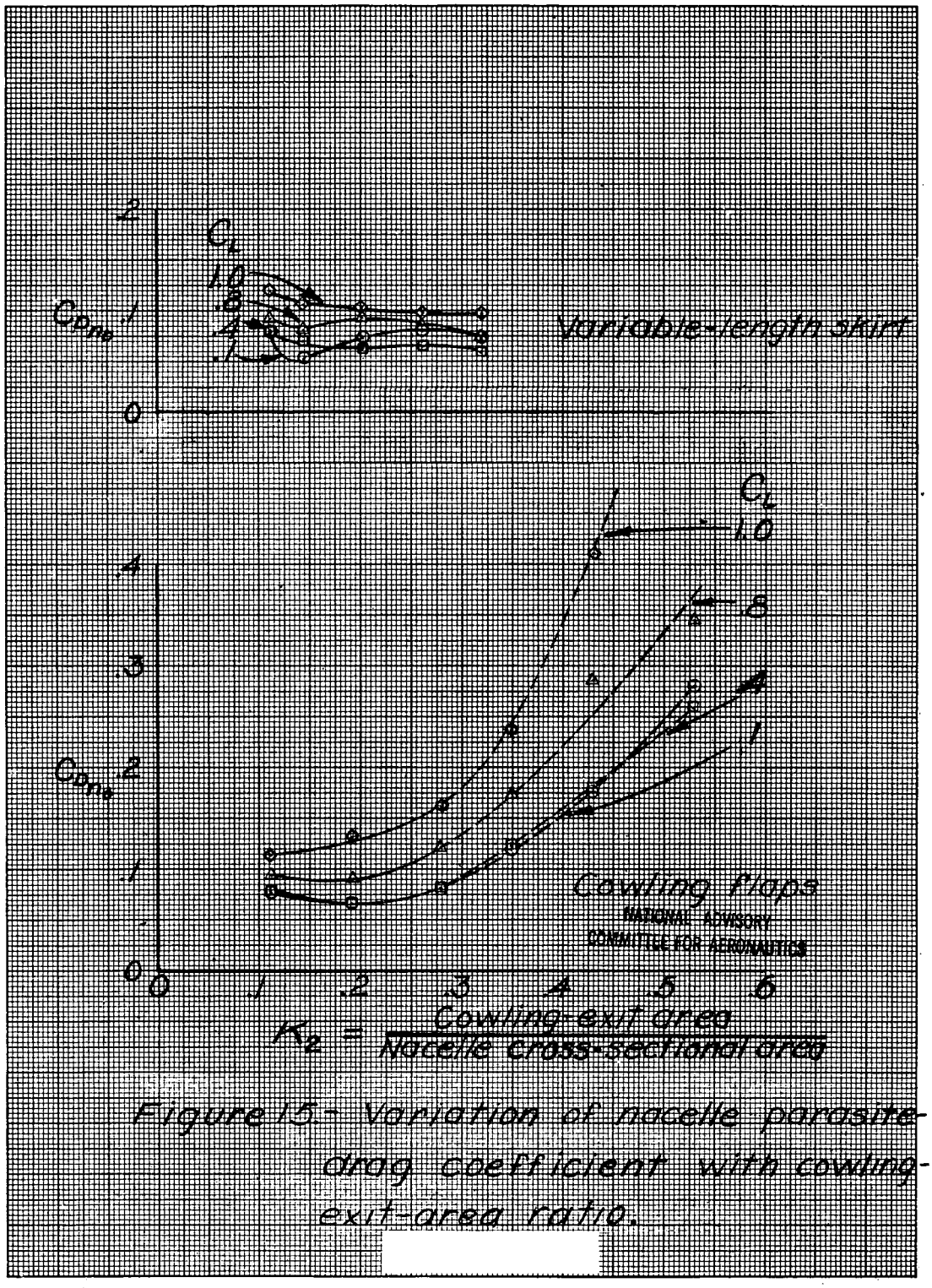

Figure 15.- Variation of nacelle parasite-drag coefficient with cowling-exit-area ratio.

L-638

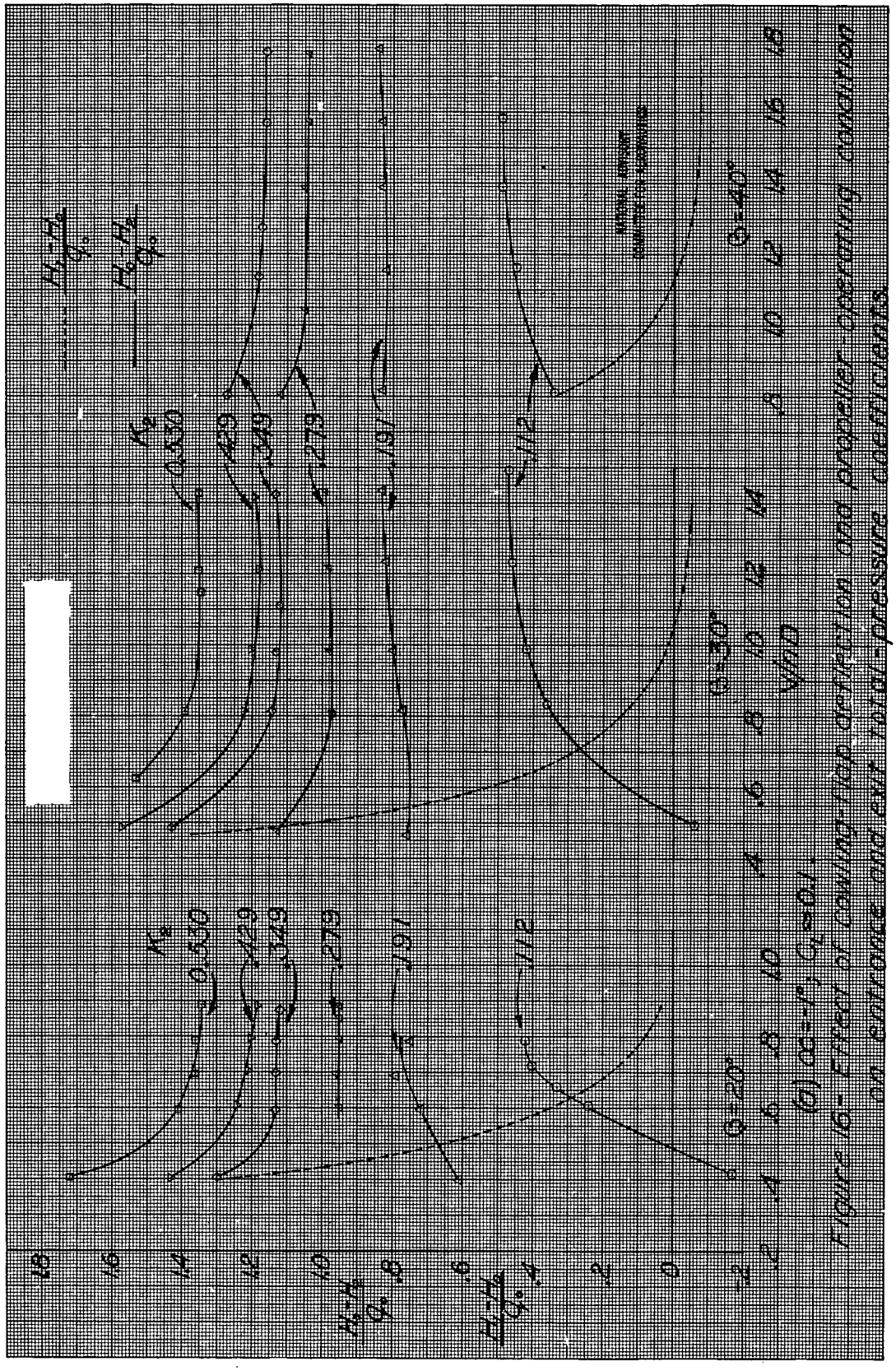

Figure 16.- Effect of compressibility on aerodynamic and propeller characteristics of an airplane model with propeller operating at high pressure coefficients.

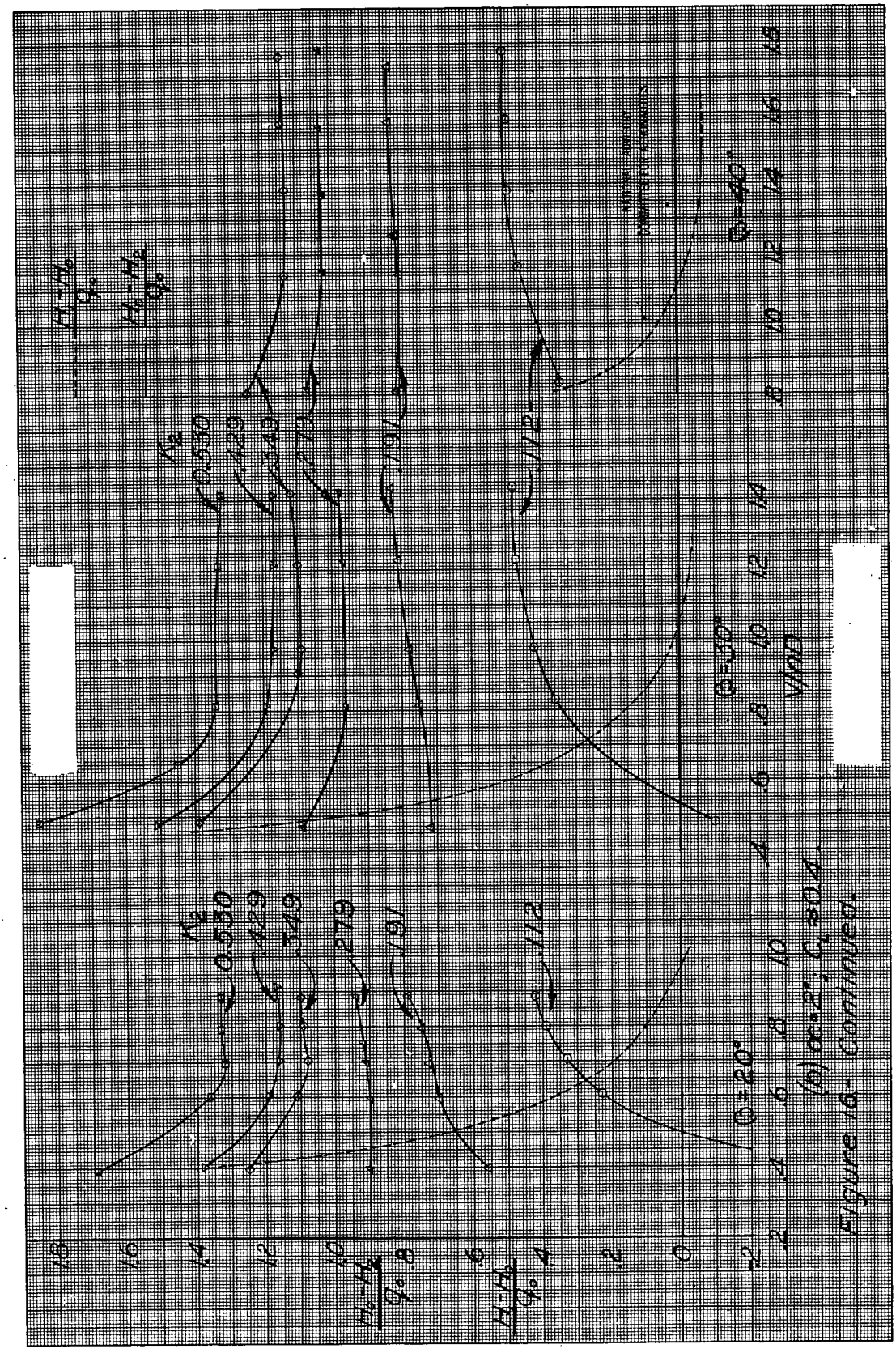
Flaps retracted
Flaps deflected
Wing
Fuselage
Elevator
Stabilizer
Fin
Rudder
Tailplane
Control surfaces
Engine nacelles
Undercarriage
Propeller
Cowling
Canopy
Windscreen
Pilot
Seat
Instrument panel
Control column
Rudder pedals
Throttle quadrant
Trim tab
Aileron
Flap
Slat
Spoiler
Dive brake
Leading edge
Trailing edge
Root
Tip
Span
Chord
Area
Aspect ratio
Taper ratio
Sweep
Dihedral
Incidence
Camber
Thickness
Fineness ratio
Wetted area
Reference area
Lift coefficient
Drag coefficient
Pitching moment coefficient
Rolling moment coefficient
Yawing moment coefficient
Side force coefficient
Lift
Drag
Thrust
Weight
Velocity
Mach number
Reynolds number
Angle of attack
Angle of sideslip
Angle of yaw
Angle of pitch
Angle of roll
Angle of incidence
Angle of dihedral
Angle of sweep
Angle of taper
Angle of camber
Angle of thickness
Angle of fineness ratio
Angle of wetted area
Angle of reference area
Angle of lift coefficient
Angle of drag coefficient
Angle of pitching moment coefficient
Angle of rolling moment coefficient
Angle of yawing moment coefficient
Angle of side force coefficient
Angle of lift
Angle of drag
Angle of thrust
Angle of weight
Angle of velocity
Angle of Mach number
Angle of Reynolds number

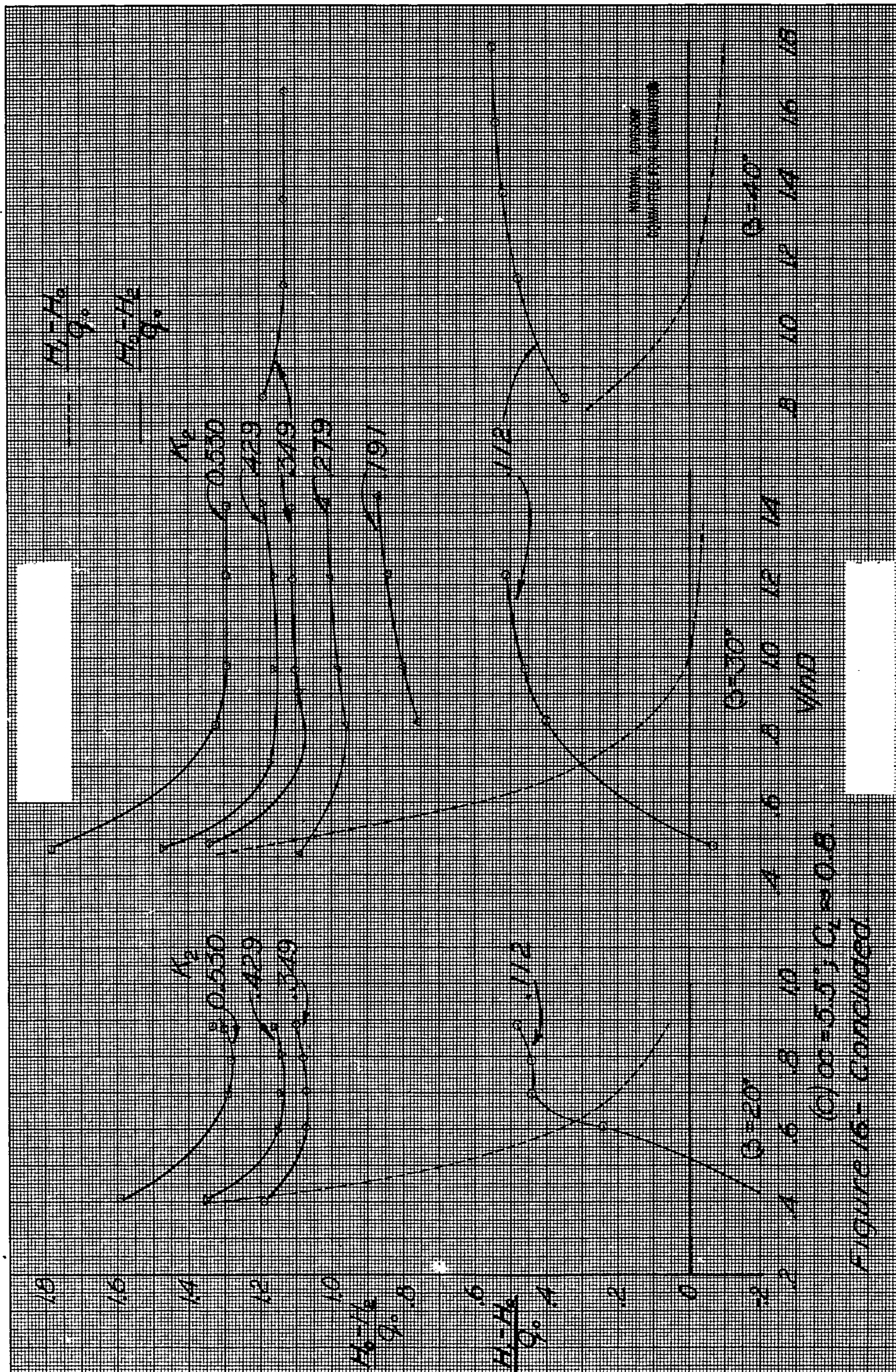

(c) $\alpha=5.5°$; $C_L=0.6$.

Figure 16- Concluded.

L-638

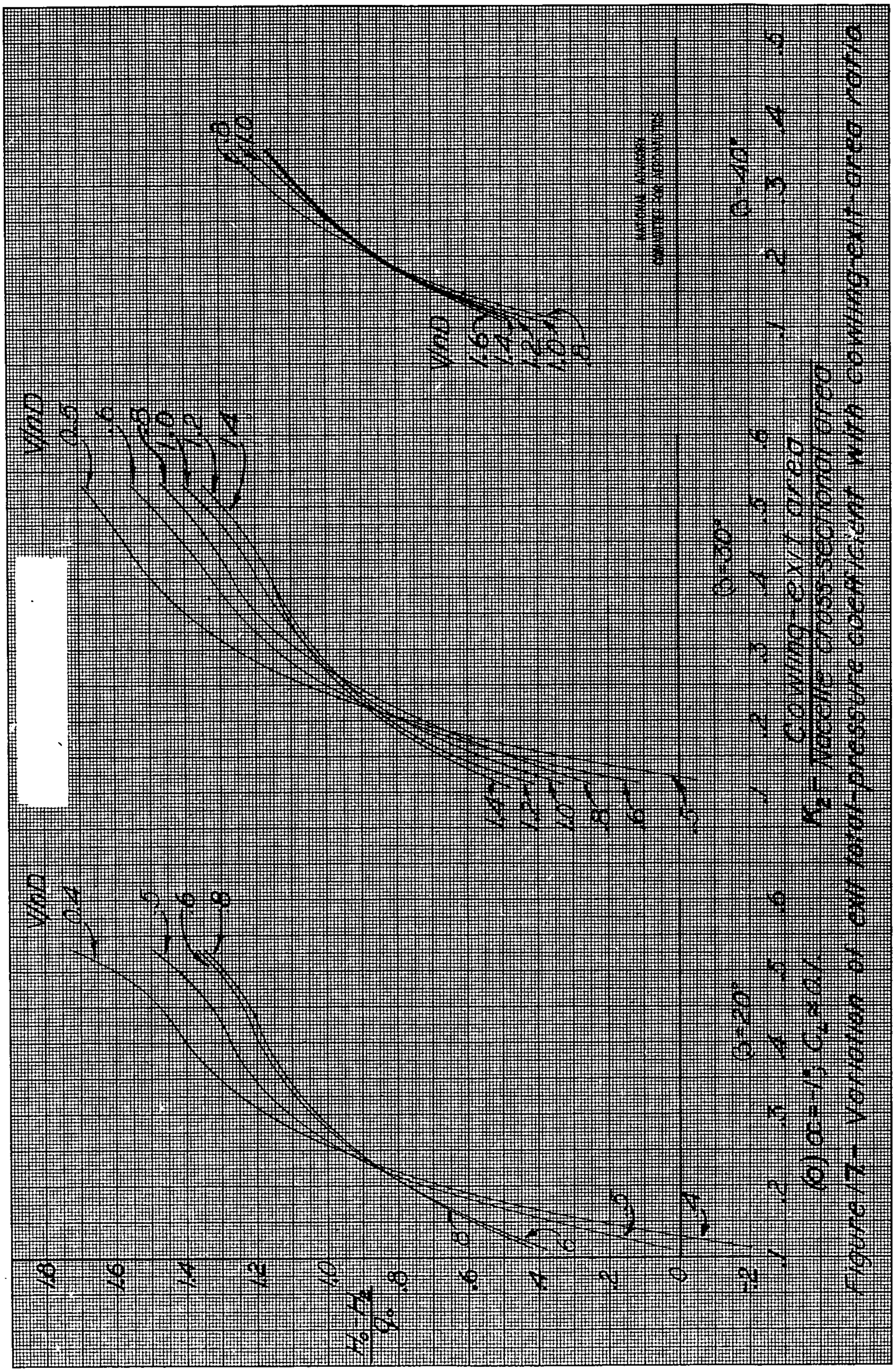

(a) α = -1°, $C_L \approx 0.1$.

Figure 17.- Variation of exit total-pressure coefficient with cowling-exit-area ratio.

L-638

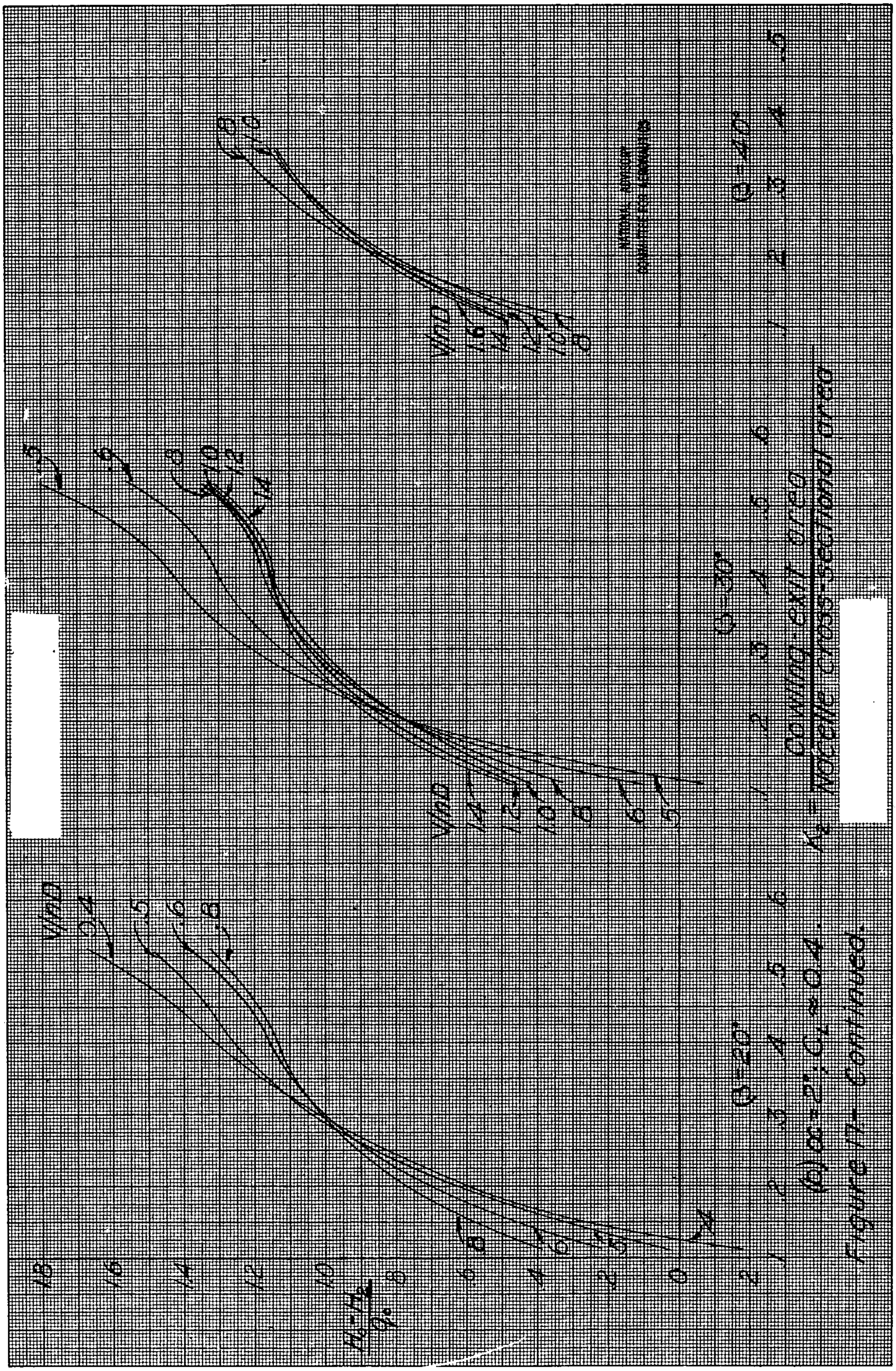

(b) $\alpha = 2°$; $C_L \approx 0.4$.

Figure 17- Continued.

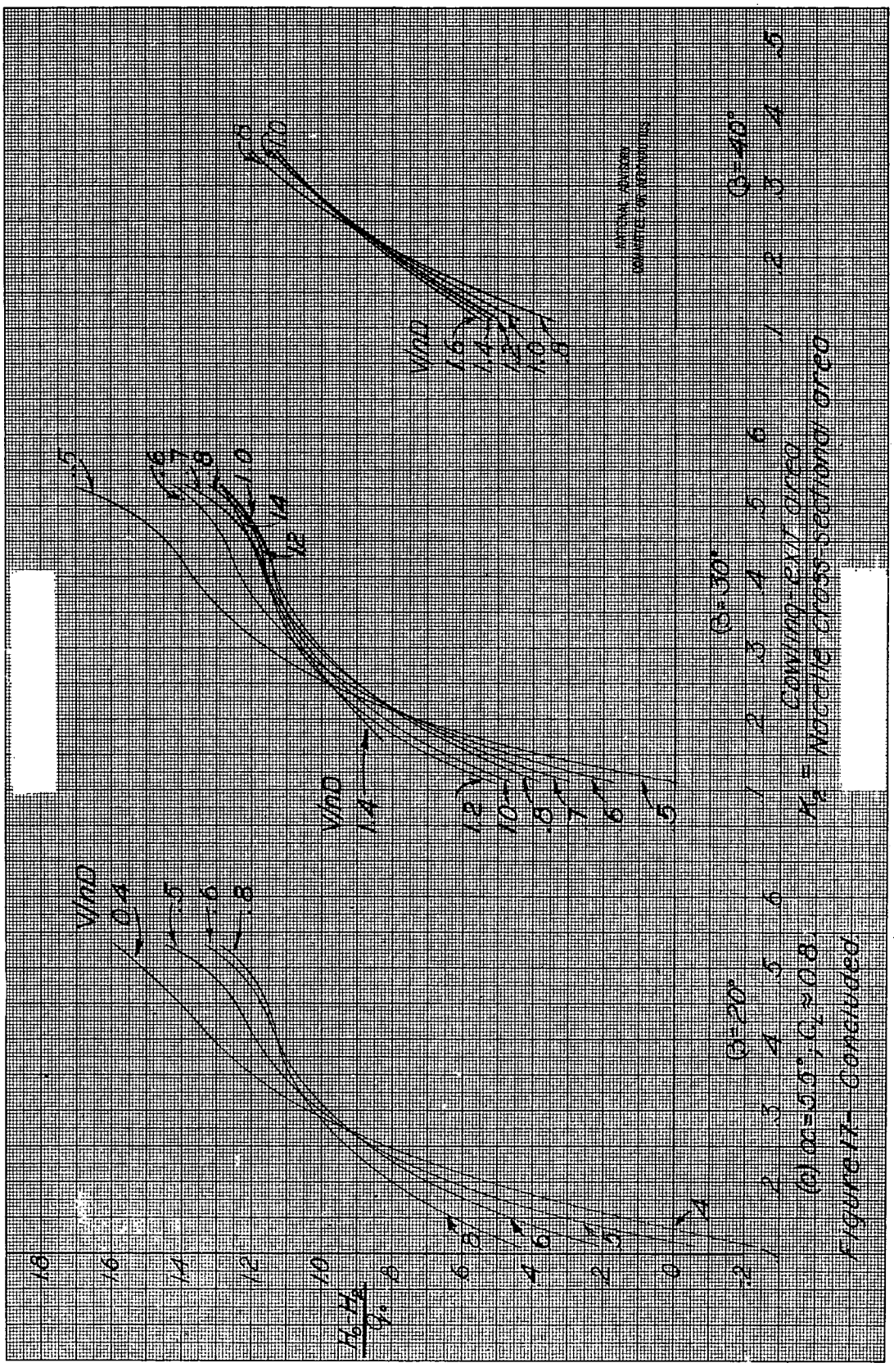
NATIONAL ADVISORY COMMITTEE FOR AERONAUTICS
Figure 17c.- Concluded.

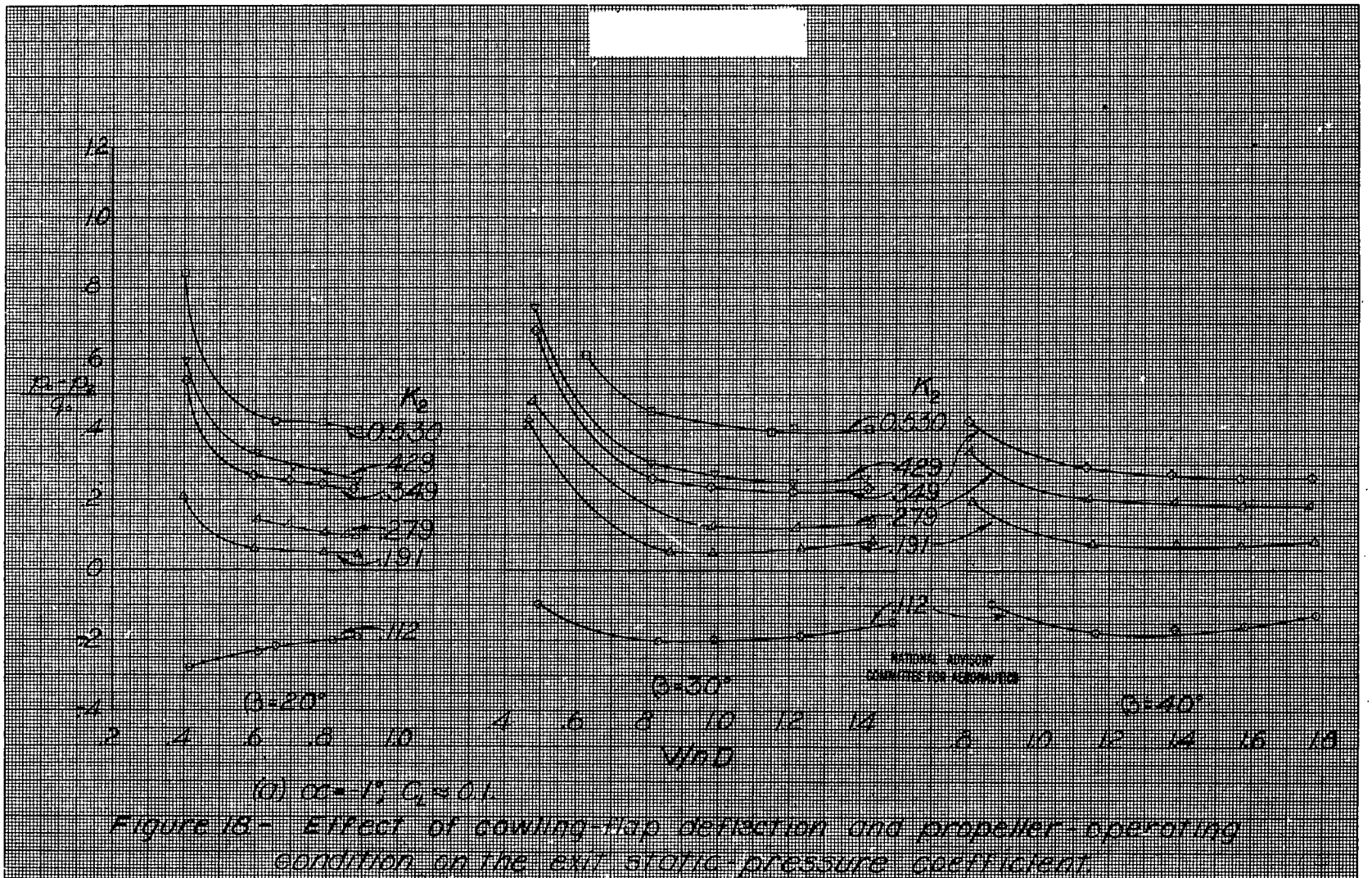

(a) $\alpha=-1°$, $C_L=0.1$.

Figure 18.- Effect of cowling-flap deflection and propeller operating condition on the exit static-pressure coefficient.

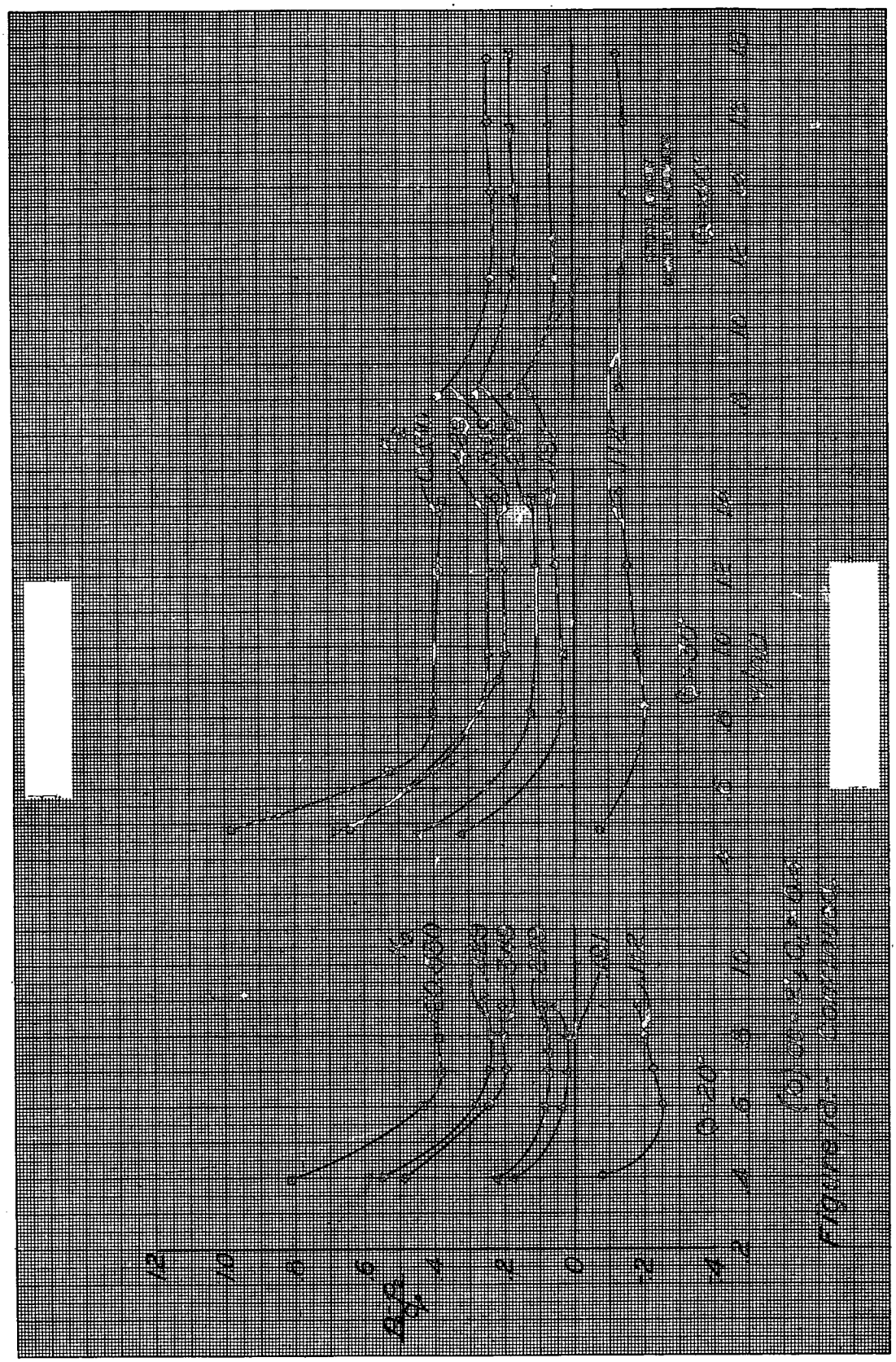

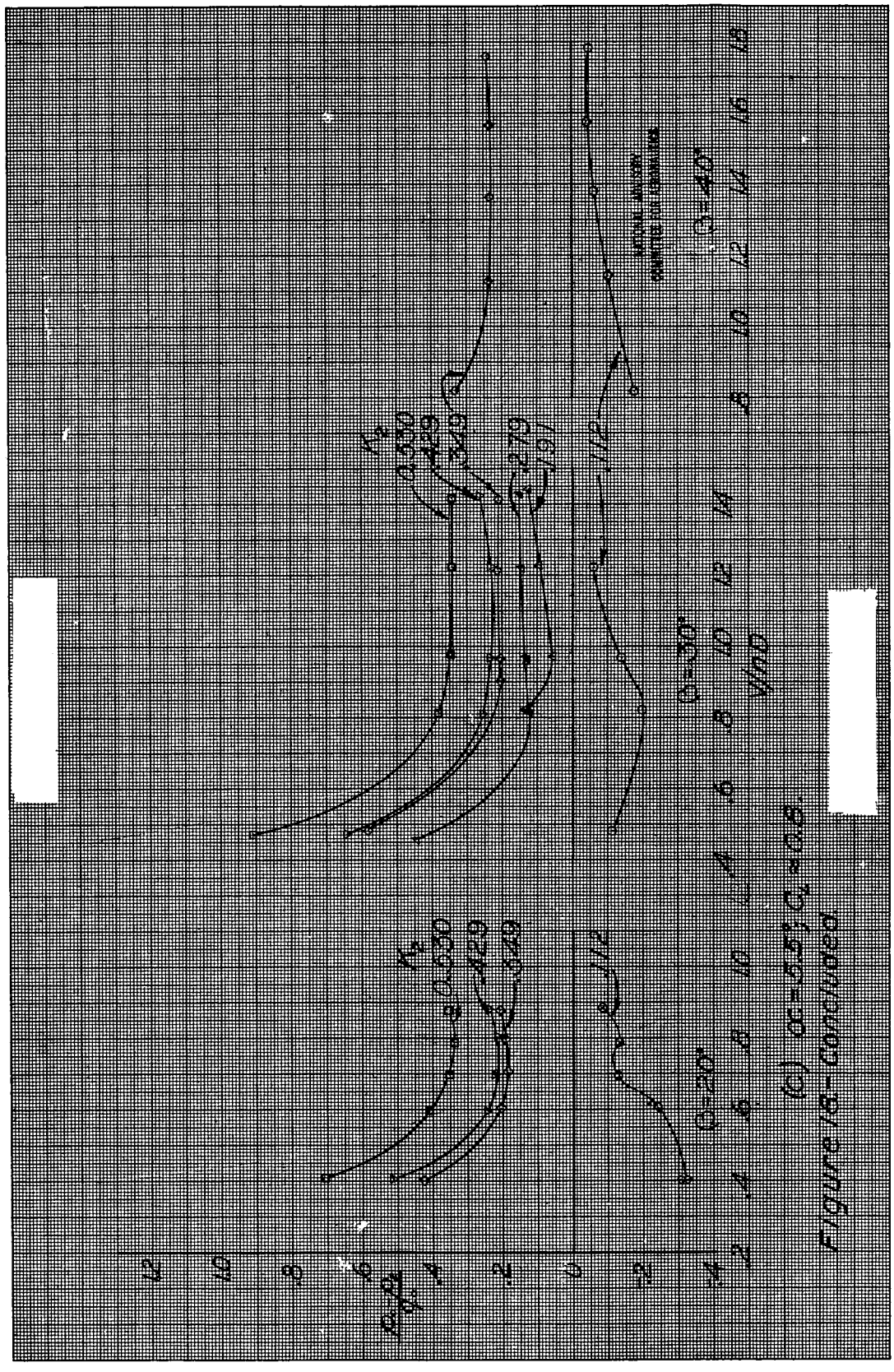
Figure 18.- Concluded.
(c) $a_r = 2.5$; $C_{m_{cg}} = 0.25$.
α, deg
C_L
C_D
C_m
$C_{m_{cg}}$
$C_{m_{ac}}$
$C_{m_{cg}} = C_{m_{ac}} + C_L \left(\frac{x_{cg}}{c} - \frac{x_{ac}}{c}\right)$
$\frac{x_{cg}}{c} = 0.25$
$\frac{x_{ac}}{c} = 0.25$
$C_{m_{ac}} = 0.000$
$C_{m_{cg}} = 0.250 C_L$
Wing alone
Wing-tail combination
i_t
δ_e
$\frac{x_{ac}}{c}$
$C_{m_{ac}}$
$C_{m_{cg}}$
$\frac{x_{cg}}{c}$

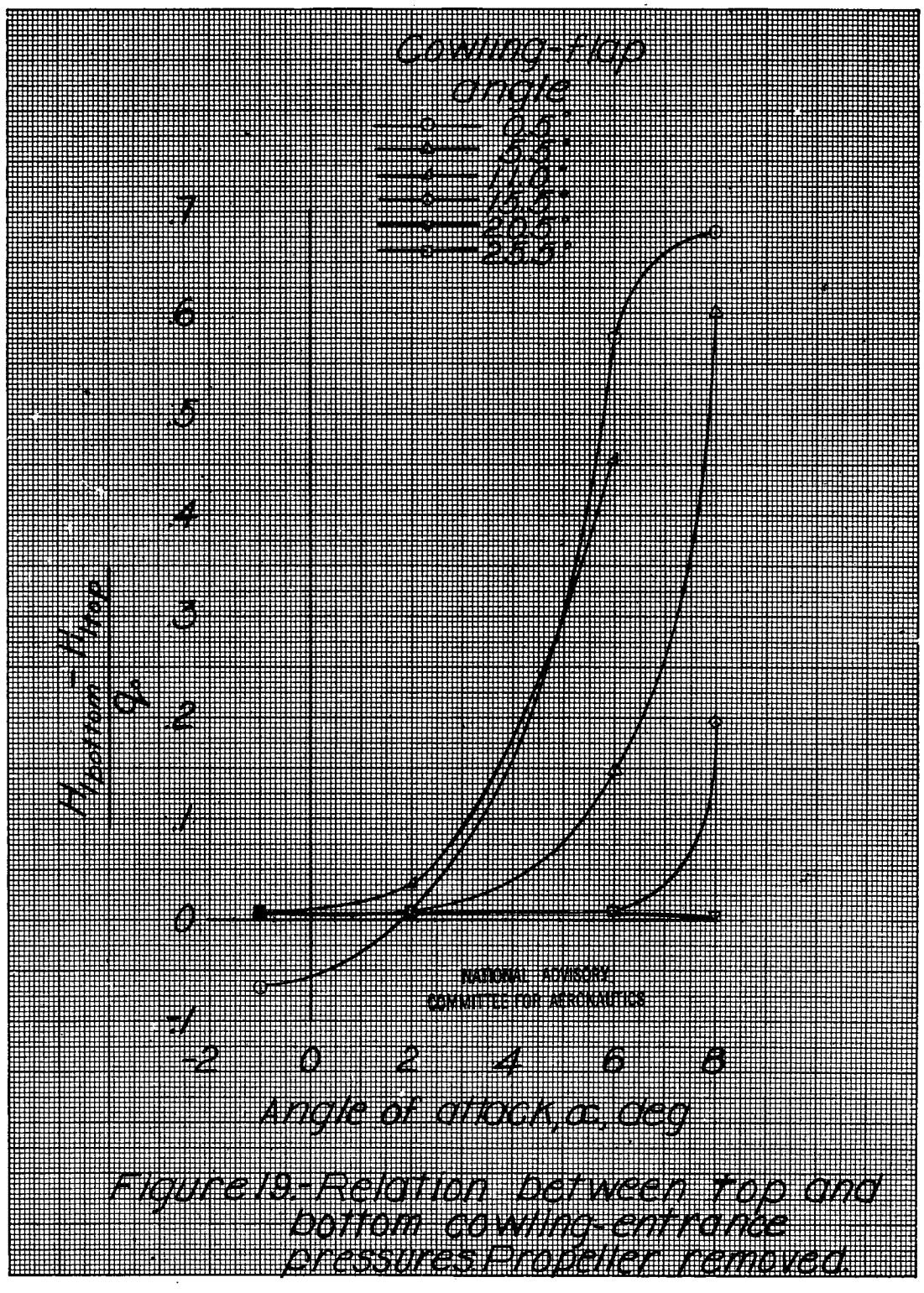

Figure 19.- Relation between top and bottom cowling-entrance pressures. Propeller removed.

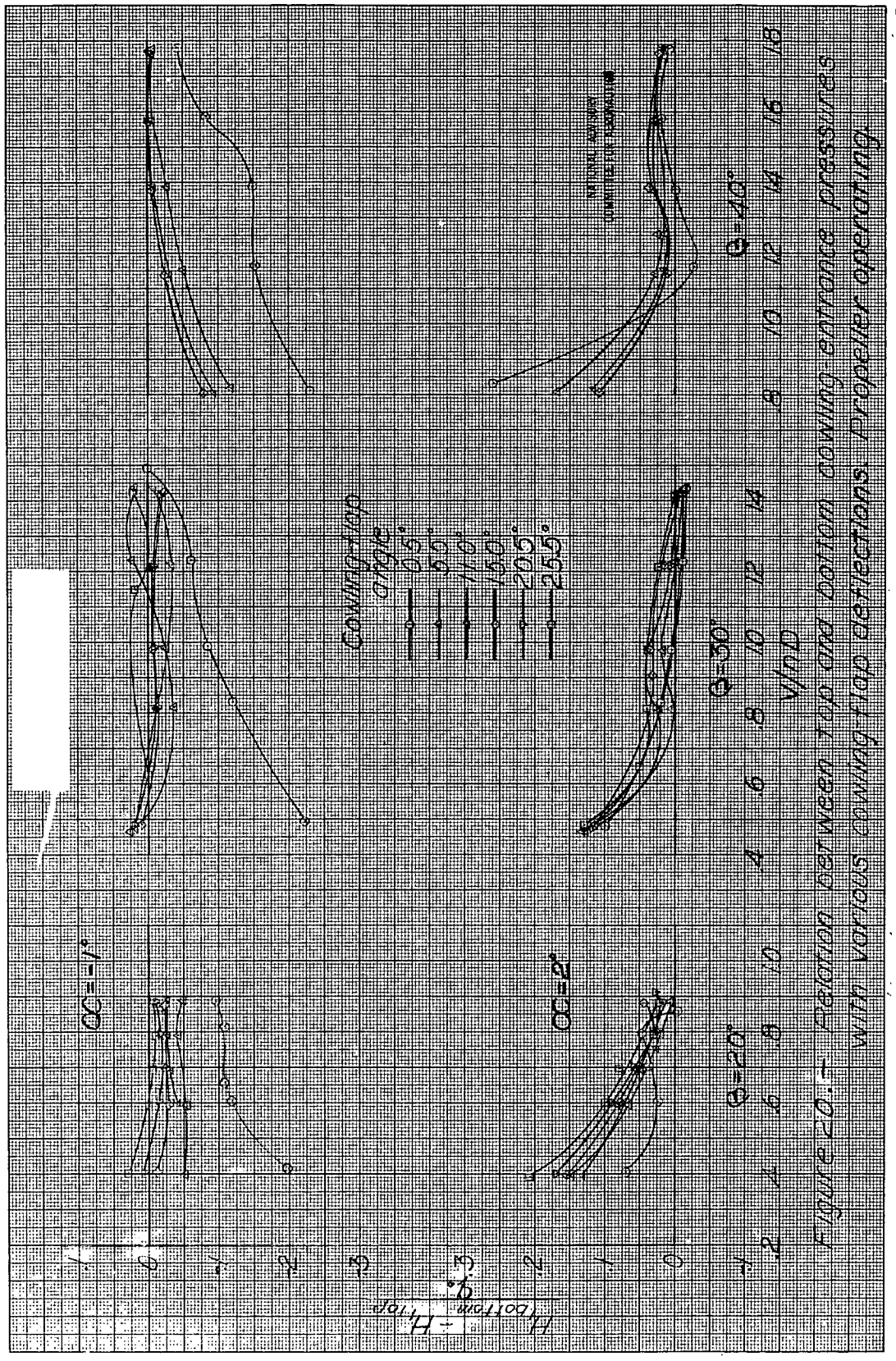
Figure 20.- Relation between top and bottom cowling drag coefficients with various cowling flap deflections. Propeller operating.
NATIONAL ADVISORY COMMITTEE FOR AERONAUTICS
δ_f=0°
δ_f=15°
δ_f=30°
δ_f=45°
δ_f=60°
Cowling flap angle
55°
155°
205°
255°
$C_{D_{bottom}}$
$C_{D_{top}}$
V/nD

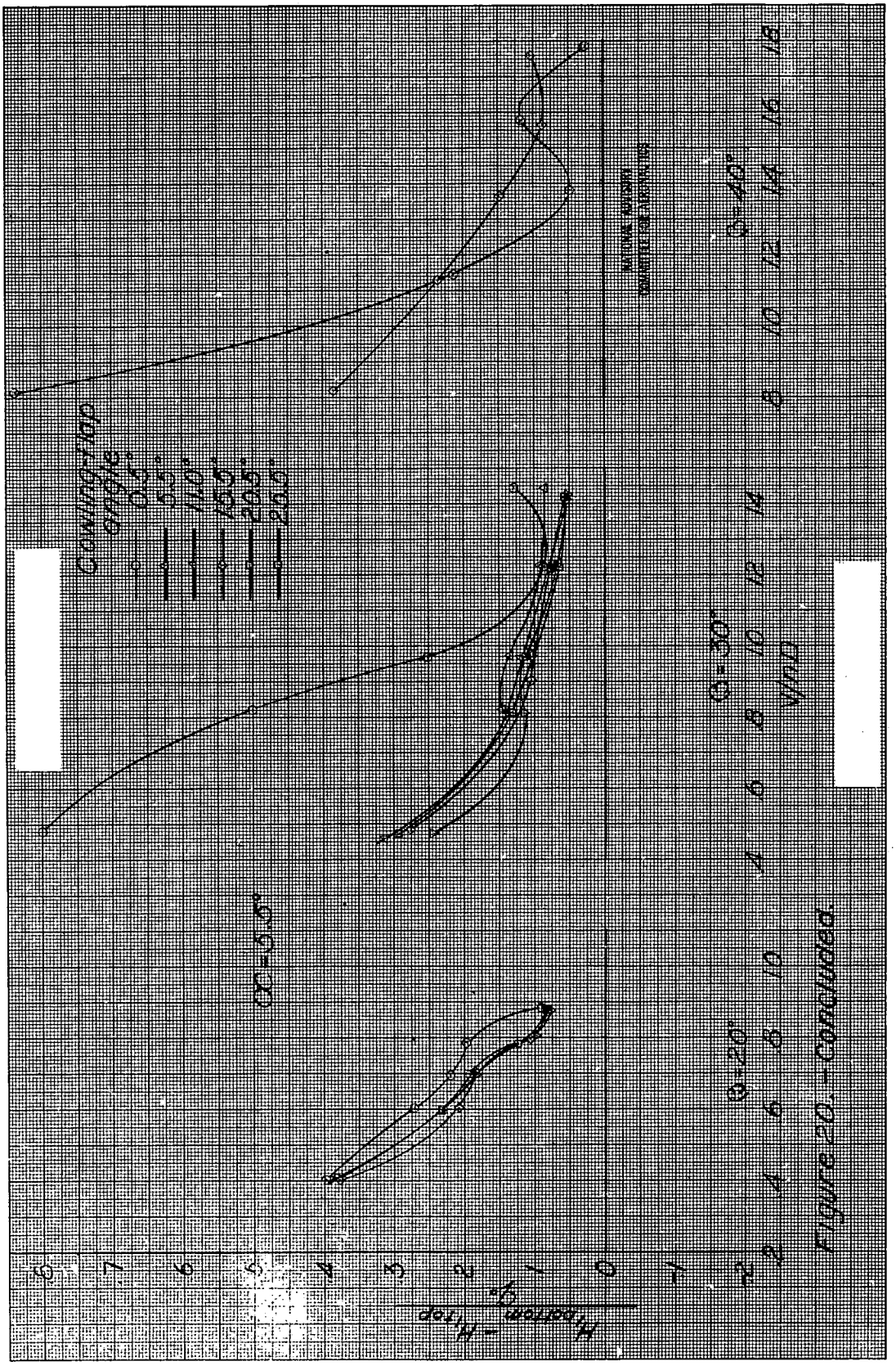
Figure 20.- Concluded.
$\alpha = 30°$
$\alpha = 20°$
$\alpha = 10°$
$\alpha = 0°$
$\alpha = -5.4°$
Control deflection
$\delta_e = 0°$
$\delta_e = -5°$
$\delta_e = -10°$
$\delta_e = -15°$
$\delta_e = -20°$
C_m
C_L
$\frac{h_{bottom} - h_{top}}{b}$

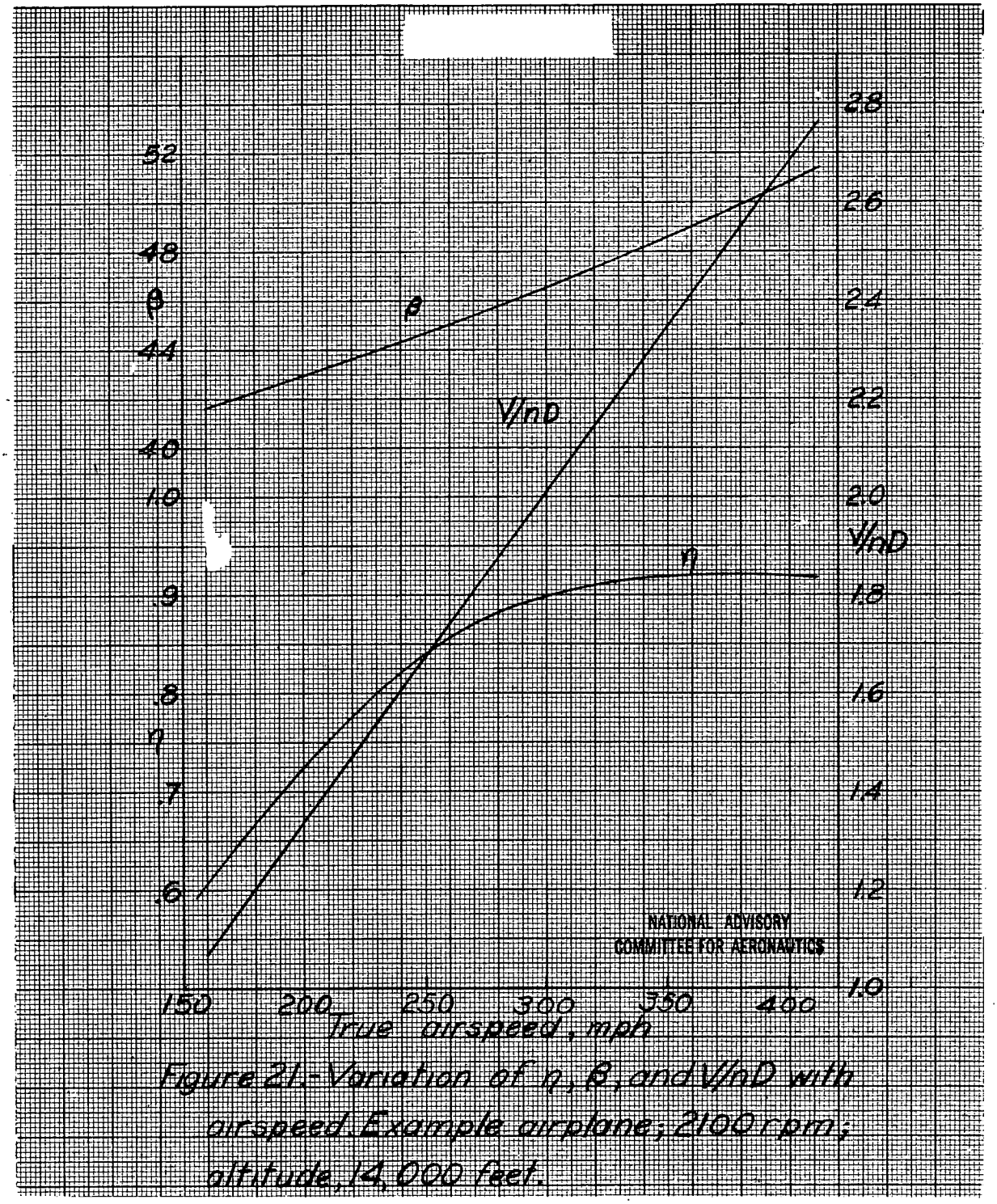

Figure 21.- Variation of η, θ, and V/nD with airspeed. Example airplane; 2100 rpm; altitude, 14,000 feet.

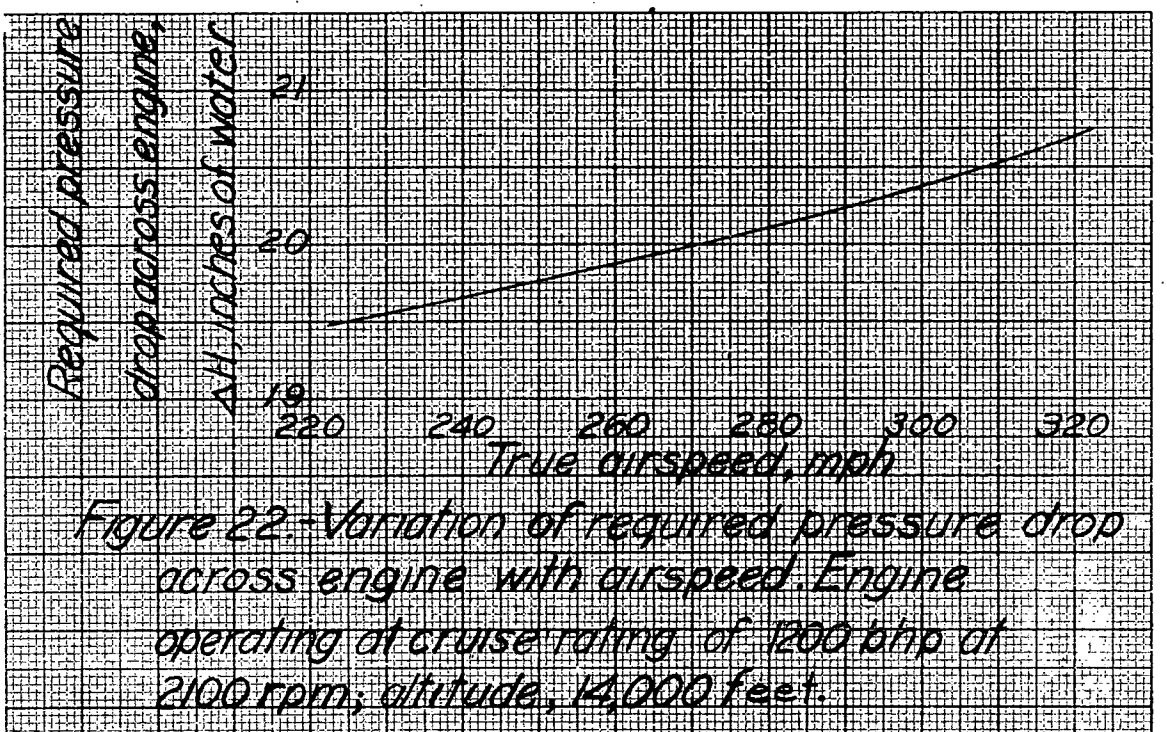

Figure 22.-Variation of required pressure drop across engine with airspeed. Engine operating at cruise rating of 1200 bhp at 2100 rpm; altitude, 14,000 feet.

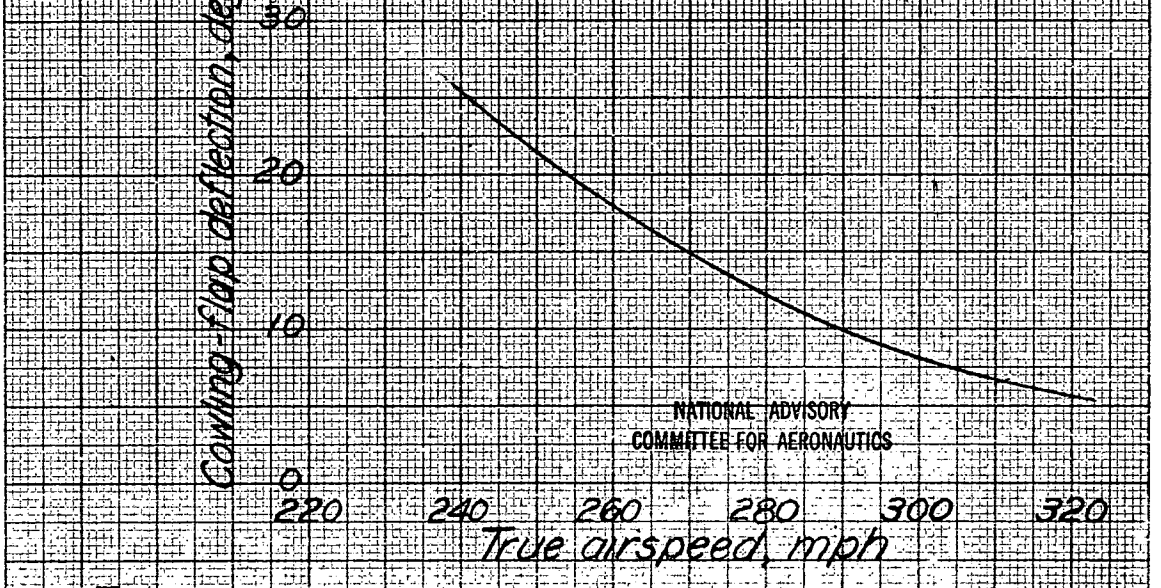

Figure 23.-Variation of required cowling-flap deflection with airspeed. Conventional engine-cooling system; engine operating at cruise rating of 1200 bhp at 2100 rpm; altitude, 14,000 feet.

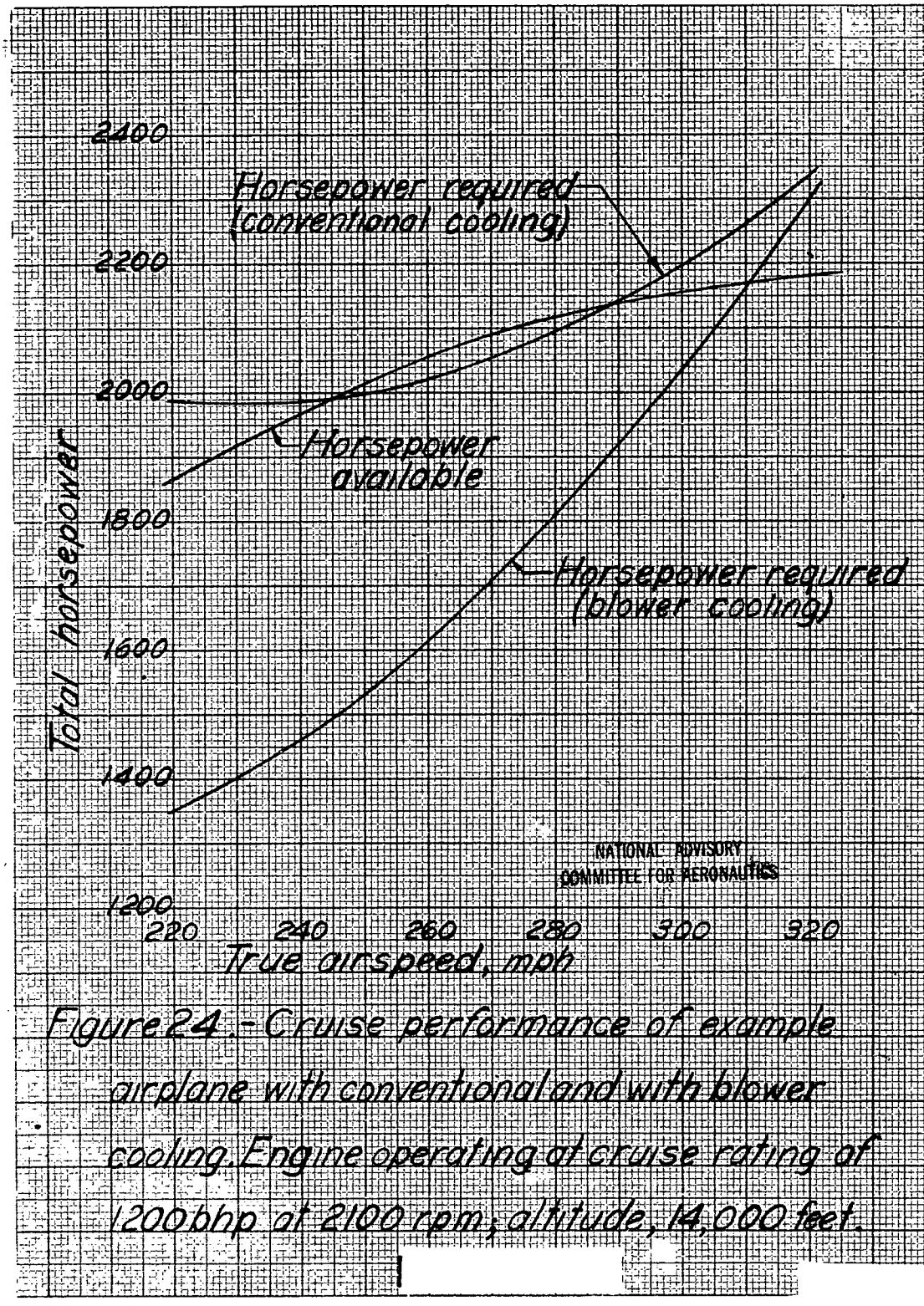

Figure 24.- Cruise performance of example airplane with conventional and with blower cooling. Engine operating at cruise rating of 1200 bhp at 2100 rpm; altitude, 14,000 feet.